

NISTIR 89-4073



Mechanical Property Enhancement in Ceramic Matrix Composites

S. W. Freiman, D. C. Cranmer, E. R. Fuller, Jr., and W. Haller

U.S. DEPARTMENT OF COMMERCE
National Institute of Standards and Technology
(Formerly National Bureau of Standards)
Ceramics Division
Gaithersburg, MD 20899

M. J. Koczak, M. Barsoum, T. Palamides, and U. V. Deshmukh

Department of Materials Engineering
Drexel University
Philadelphia, PA 19104

INTERIM REPORT

January 1989

Issued April 1989

This program supported by the Strategic Defense Initiative
Office/Innovative Science and Technology under ONR Contract
Contract Number: N00014-86-F-0096

QC
100
.U56
89-4073
1989
C.2

**NATIONAL INSTITUTE OF STANDARDS &
TECHNOLOGY**
Research Information Center
Gaithersburg, MD 20899

NISTR
QC100
. 456
no. 89-4073
1989
c. 2

NISTIR 89-4073

Mechanical Property Enhancement in Ceramic Matrix Composites

S. W. Freiman, D. C. Cranmer, E. R. Fuller, Jr., and W. Haller

U.S. DEPARTMENT OF COMMERCE
National Institute of Standards and Technology
(Formerly National Bureau of Standards)
Ceramics Division
Gaithersburg, MD 20899

M. J. Koczak, M. Barsoum, T. Palamides, and U. V. Deshmukh

Department of Materials Engineering
Drexel University
Philadelphia, PA 19104

INTERIM REPORT

January 1989
Issued April 1989



National Bureau of Standards became the National Institute of Standards and Technology on August 23, 1988, when the Omnibus Trade and Competitiveness Act was signed. NIST retains all NBS functions. Its new programs will encourage improved use of technology by U.S. industry.

This program supported by the Strategic Defense Initiative Office/Innovative Science and Technology under ONR Contract Contract Number: N00014-86-F-0096

U.S. DEPARTMENT OF COMMERCE
Robert Mosbacher, Secretary
NATIONAL INSTITUTE OF STANDARDS
AND TECHNOLOGY
Raymond G. Kammer, Acting Director

ABSTRACT

The fiber-matrix interfacial properties of several glass and ceramic matrix composites have been determined using two indentation techniques and a single fiber pull-out technique. An instrumented indenter was developed to improve the acquisition and analysis of the data. The effects of thermal expansion mismatch were determined from three model composite systems containing large SiC monofilaments using the single fiber pull-out test. An indentation push-out test was successfully used to determine the debond strength of a borosilicate matrix/SiC monofilament/carbon core material. A comparison of the various techniques for determining the fiber-matrix interfacial properties was conducted.

MECHANICAL PROPERTY ENHANCEMENT IN CERAMIC MATRIX COMPOSITES

BACKGROUND

The key parameters responsible for the stress-strain behavior and damage tolerance of fiber-reinforced ceramic composites are the fracture toughness of the matrix, the strength of the fiber/matrix interface, and the properties and distribution of the fibers themselves. Increases in the fracture resistance of the matrix and the strength of the interface are predicted to lead to an increase in the stress at which the matrix begins to microcrack. Balanced against this increase in microcracking stress is the necessity for maintaining some degree of fiber pullout in order to achieve the desired stress-strain behavior of the composite. Quantitative experimental verification of the models developed to explain composite fracture (1-5) has not yet been obtained.

The primary objective of this program is to experimentally determine the relationships between the fracture behavior of fiber-reinforced ceramic composites, the properties of the individual components, and the interface between the fiber and the matrix. A second objective is to establish mechanical test procedures appropriate for these composite systems. The increased understanding of the fracture process will be used to develop strong/damage tolerant materials.

To meet these objectives, we have examined a number of different composite systems by a number of different test procedures. Both the systems examined and the test methods used on each are shown in Table 1. The systems chosen are either model systems ($\text{Na}_2\text{O-CaO-SiO}_2$, $\text{Na}_2\text{O-B}_2\text{O}_3\text{-SiO}_2$, and $\text{CaO-TiO}_2\text{-SiO}_2$ matrices reinforced with SCS-6 SiC^1) or commercially available materials

¹Textron Specialty Materials, Lowell, Massachusetts

Table 1

Materials and Test Methods Used to Determine Fiber-Matrix Properties

<u>Test Methods</u> →	Single Fiber Pull-Out	Indentation Push-In	Indentation Push-Out
<u>Materials</u> ↓			
Na ₂ O-B ₂ O ₃ -SiO ₂ /SCS-6 SiC	X		X
Na ₂ O-CaO-SiO ₂ /SCS-6 SiC	X		
CaO-TiO ₂ -SiO ₂ /SCS-6 SiC	X		
LAS III/Nicalon SiC		X	X

(LAS III matrix reinforced with Nicalon SiC²)³. The model systems were chosen for a number of reasons including ease of fabrication, thermal expansion mismatch between fiber and matrix, and the handleability and reproducibility of the fibers.

The work performed to date is divided into three parts: 1) measurement of the fiber-matrix interfacial properties, 2) determination of thermal expansion mismatch effects on the fiber-matrix interfacial properties, and 3) development and comparison of various test methods for determining fiber-matrix interfacial properties. The interfacial properties of interest include interfacial frictional stresses and fiber-matrix debond strength, which as noted above, determine the balance between matrix microcracking, at which point environmental effects can become important, and graceful failure of the composite.

² Nippon Carbon, Tokyo, Japan

³ United Technologies Research Center, East Hartford, CT

RESULTS

Interfacial Strength Measurement Via Instrumented Indentation Testing

The method used to determine the strength of the fiber/matrix interface is based on the indentation technique described by Marshall (6). A Vickers diamond indenter is used to apply a force, F , to a fiber parallel to the fiber axis in a polished cross section of the composite. The method is an extension of Marshall's technique in that the indenter is instrumented to measure both the load applied to the fiber as well as the displacement of the diamond tip. The load-displacement curves can be used to calculate the interfacial stresses or fiber-matrix debond strength.

In our variation, a strain gage load cell and capacitance sensors are used to determine the load and displacement and recorded in real-time via computer. Typical results of applied load and displacement of the fiber versus time are shown in Figure 1. This raw data is converted to force squared (F^2) versus displacement (δ) from which the debond strength or interfacial friction stresses are calculated. The instrument can be used to perform either the indentation push-in test wherein the fiber is pushed into the matrix or an indentation push-out test wherein the fiber is pushed through the matrix. A typical plot of F^2 versus δ for the indentation push-in test is shown in Figure 2. τ_f is calculated from the slope of this plot as:

$$\tau = \frac{m}{4 \pi^2 R^3 E_f} \quad (1)$$

where m is the slope, R is radius of the fiber, and E_f is the elastic modulus of the fiber.

In the indentation push-out test, three regimes of behavior are expected and illustrated schematically in Figure 3. The first regime resembles the indentation push-in test where the Vickers diamond is only in contact with the

fiber and the fiber is not completely debonded from the matrix but is moving in the matrix. The second regime occurs when the fiber has completely debonded from the matrix and is slipping along its entire length through the matrix. In Figure 3, this regime is denoted by the plateau region. Although shown as a flat plateau, there should be a slight decrease in F^2 versus δ as the length of the fiber in the matrix becomes smaller. In practice, for at least some materials, this decrease is not observed. The third regime occurs when the diamond makes contact with the matrix and the force increases significantly with little change in displacement. In the initial regime, τ_f can be determined from the slope of F^2 versus δ according to equation 1. In the plateau region, τ_f or τ_d are determined from the value of the force at the plateau according to:

$$\tau = \frac{F}{2 \pi R t} \quad (2)$$

where t is the thickness of the specimen.

For large monofilaments, such as Textron's SCS-6 SiC, where the SiC is deposited on a carbon core, two plateaus are expected. The first occurs when the carbon core (33 μm diameter) slips in the SiC; the second occurs when the SiC fiber (about 140 μm diameter) slips in the matrix.

An alternative method for determining the strength of interfaces is the single fiber tensile test. This test gives a direct measure of the interface strength (7-9) and provides information on both the debonding and pull-out processes occurring in composites. In spite of these advantages, single fiber pull-out tests have been used only recently for glass matrix systems (10-12). This test is discussed in more detail in the next section, as the results obtained this year with this method are related to understanding the effects of thermal expansion mismatch.

Effects of Thermal Expansion Mismatch on Interfacial Properties

In the absence of a chemical bond across the interface, or if an existing bond is broken, the resistance to fiber pull-out is mainly from interfacial frictional stresses, τ_f . If the matrix shrinks more than the fiber (due to thermal expansion), a residual compressive stress acting at the interface is produced, which depends on the elastic properties of the fiber and matrix, the difference in thermal expansion between the fiber and matrix, and the temperature difference between the glass strain point (T_s) and room temperature (T_{rt}). When $\alpha_{glass} > \alpha_{SiC}$, a larger thermal expansion coefficient difference should lead to a larger compressive stress, and thus to a higher resistance to pull-out. To confirm this hypothesis, experimental data were collected on both soda-lime-silica glass/SiC fiber and calcia-titania-silica glass/SiC fiber systems for comparison with data [10] on a borosilicate glass/SiC fiber system. The SiC fiber was the large diameter SCS-6, chosen because of its ready availability, reproducibility of properties, and handleability after sample fabrication. The single fiber pull-out test was used to determine the interface properties because of the ease of sample fabrication and the ability to determine both debond strengths and interfacial frictional stresses. The coefficient of thermal expansion for each material is shown in Table 2. Using this information, τ_f should increase in the order $CaO-TiO_2-SiO_2 \rightarrow Na_2O-B_2O_3-SiO_2 \rightarrow Na_2O-CaO-SiO_2$.

Table 2

Thermal Expansion Coefficients of Matrices and Fiber

SiC Monofilament	$26 \times 10^{-7} \text{ } ^\circ\text{C}^{-1}$
Soda-Lime-Silica Glass	82×10^{-7}
Borosilicate Glass	32×10^{-7}
Calcia-Titania-Silica	13×10^{-7}

Single fiber pull-out samples were fabricated by sandwiching SiC monofilaments between borosilicate glass plates and heating under dead weight loading corresponding to 14-21 KPa pressure. Molybdenum sheets were placed between the dead weight and the glass plates to prevent adhesion during fabrication. The entire assembly was immersed in graphite powder to prevent oxidation of the fibers. Industrial grade argon was kept flowing through the furnace. The samples were held at 760°C for 60 min to obtain good flow of the glass around the monofilament. A schematic of the finished samples is shown in Figure 4. Different embedded lengths were obtained by varying the length of the monofilament between the plates. Individual samples were loaded in uniaxial tension on a screw-driven universal test machine⁴. The samples were gripped using swivel hooks attached to ball joints to facilitate alignment of the fiber with the stress axis. Samples were pulled at a rate of 0.05 cm/min. The embedded length was determined from the force-displacement curves (Figure 5), since accurate optical measurements prior to testing could not be made due to uncertainty in where the monofilament emerged from between the glass plates.

Two types of force-displacement curve were observed in the soda-lime-silica glass/SiC fiber system as shown in Figure 6. In both cases, the load increased linearly with displacement until the fiber debonded from the matrix. In the first case, there was a sharp drop in load, followed by pull-out of the fiber. In the second case, the load decreased gradually from the maximum while the fiber pulled out. The incidence of "stick-slip" behavior during pull-out was much less frequent than in the borosilicate glass/SiC system [4], suggesting the presence of a lubricating layer between the fiber and the soda-lime-silica matrix.

⁴ Instron Corp., Canton, MA.

The maximum force required to initiate pull-out of the fiber is plotted vs embedded length in Figure 7. Although there is considerable scatter in the data, it can be seen that the pull-out force increases with increasing embedded length as long as the fiber strength is not exceeded. Some of the scatter may be due to non-uniform flow of glass around the fiber, leading to an air gap at the interface, and therefore reduced contact area and pull-out force. Also plotted in Figure 7 are the loads at which only frictional forces are acting on the interface. The difference between the maximum load and the frictional load is not constant. To confirm that the first load drop is due to debonding, several samples were unloaded following the initial load drop, then reloaded. Upon reloading, pull-out was observed at the same load where unloading had occurred, showing that the fiber-matrix bonds were in fact broken initially and that only frictional stress was operating at the interface. Occasionally, after reloading, a very small load drop was observed which is attributable to the difference between the static and dynamic coefficients of friction. The stability of τ during pull-out over a wide range of instantaneous embedded length is demonstrated in Figure 8.

Table 3 shows calculated values for τ for the soda-lime-silica, calcia-titania-silica, and borosilicate glass systems. The large standard deviation

Table 3

Shear Stresses and Coefficients of Friction for Glass/SiC Systems

	Calcia-titania-silica glass	Borosilicate glass	Soda-Lime-Silica Glass
$\Delta\alpha$ ($10^7/^\circ\text{C}$)	-13.0	6.2	56
τ_d (MPa)	3.1	11.1 ± 3.2	18.7
τ_f (MPa)	3.1	3.6 ± 0.7	13.9 ± 4.1
μ	Not measured	0.72 ± 0.36	0.10 ± 0.03

for the soda-lime-silica system is believed to be due to variations in processing conditions. Friction coefficients, μ , were also obtained from this data. For the soda-lime-silica system, μ was calculated to be 0.10 ± 0.03 ; for the borosilicate system, μ is 0.72 ± 0.36 . The frictional stress acting at the interface may now be calculated as the product of μ and σ_n , where $\sigma_n = \sigma_0 - k\sigma_f$, σ_f being the axial stress corresponding to the frictional force and $k\sigma_f$ representing the reduction in σ_n due to Poisson's contraction. For the soda-lime-silica system, τ_f was calculated to range from 4-20 MPa, for the borosilicate system, it was in the range from 2-3 MPa, and for the calcia-titania-silica system, it was ≈ 3 MPa. It can therefore be seen that increasing the thermal expansion mismatch between the fiber and the matrix to increase the compressive stress on the fiber yields a greater resistance to fiber pull-out, and should result in a more damage tolerant material, provided the increased compressive stress does not result in microcracking in the matrix surrounding the fiber.

Comparison of Techniques for Determining Fiber-Matrix Properties

No one material lends itself to testing using all three methods (indentation push-in, indentation push-out, and single fiber pull-out) described above, and no single test method provides all of the information desired on interfacial mechanical properties. The reasons for this are as follows. In a single fiber pull-out test, the combination of a small fiber diameter (10-20 μm) for materials such as Nicalon SiC, high temperature ($>700^\circ\text{C}$) processing required to obtain an acceptable sample geometry, and handling to set up each experiment makes it difficult at best to perform the test on a large enough number of samples. In the indentation push-in test, the large monofilaments tend to crush or split rather than slide, thus

obliterating the indentation impressions and yielding inaccurate displacement measurements. To date, no work has been published regarding the use of the indentation push-out test on layered fibers such as SiC deposited on C or W cores. In view of these problems, two model composite systems were chosen which were amenable to measurements by more than one technique. The model systems examined included the borosilicate glass/SCS-6 and the LAS III/Nicalon. The borosilicate glass system was tested using the pull-out and indentation push-out techniques, while the glass-ceramic system was tested using the two indentation techniques.

As noted in the previous section, single fiber pull-out tests give the most direct measure of the interface strength, but the tests performed to date have only been conducted on monofilaments. Indentation testing is a relatively new technique for determining fiber/matrix interfacial properties. Interfacial frictional stresses of 2.5 ± 0.9 MPa have been measured for LAS-III/Nicalon SiC-reinforced glass-ceramic, but the method requires precise measurement of very small indentation sizes, potentially a significant source of error. For the results to be valid, the specimen thickness must be large compared to the diameter of the fiber. Additional studies by Marshall and Oliver [13] refined the method by using a pyramidal indenter at ultralow loads (< 0.12 N). In this method, the indenter is instrumented to provide independent determinations of force applied to the fiber and displacement of the fiber in the matrix. The revised method permits examination of both debonding and frictional sliding in a SiC/glass-ceramic composite. Values of r_f on the order of 3.5 MPa were obtained on this material, in good agreement with the initial measurements using the Vickers diamond. One particular aspect of this method which limits its use is the special apparatus required to apply very small loads, although efforts are currently being made to expand

the load range which can be applied [14]. While most of the work on the indentation push-in test has been conducted using a standard Vickers diamond geometry, Mandell et al [15] have shown that the shape of the indenting diamond can be changed to increase the amount of sliding which can be observed.

The materials for the indentation tests were either obtained from commercial sources or made by hot pressing a sample of SiC/borosilicate glass at 800°C for 30 minutes at about 14 KPa. Specimens for indentation included 1 mm and 2 mm thick multifilament SiC/glass-ceramic and 0.3 mm thick monofilament SiC/borosilicate glass. The samples were at least partially flat and polished so that the capacitance probes did not have to be adjusted frequently. A 50 g load was used for the SiC/glass-ceramic material, and the loads ranged from 130 to 150 g for the SiC/borosilicate material. Based on the debond strength of the SiC/glass, as determined from the single fiber pull-out test (9 MPa), loads < 140 g should exhibit a single plateau of the core slipping in the SiC while loads > 140 g should exhibit both plateaus.

As noted above, which value of τ is measured depends on the test method employed as well as the material being tested. It is expected that the single fiber pull-out test will provide information on both debonding strength and frictional stresses, while the push-in test will measure frictional stresses only. The push-out test could measure either or both debond strength or frictional stress, depending on the material and the indenter geometry.

The types of force-displacement curves obtained from the single fiber pull-out test are described in the previous section. In both cases, the load increased linearly with displacement until the fiber debonded from the matrix. In the first case, there was a sharp drop in load, followed by pull-out of the fiber. In the second case, the load decreased gradually from the maximum

while the fiber pulled out. The two types of curves may indicate two types of interface failure. A sudden drop indicates catastrophic failure of the entire interface whereas the smoother curve indicates a more gradual, incremental failure of the interface.

The values of τ_f measured using the single fiber pull-out test for the SiC/borosilicate system are lower than those obtained by Goettler and Faber [12] (12.5 MPa), but the analytical methods were different, as were the specimen fabrication procedures. When the data of Deshmukh and Coyle [10] for SiC reinforced borosilicate glass are examined using the analysis of Goettler and Faber, a value of τ_f of 22 MPa is obtained. When the expected residual stresses are taken into account, a value of τ_0 between 7 and 18 MPa is found, depending on the choice of friction coefficient (0.2 vs 0.72). A friction coefficient of 0.72 is the value taken from reference 10, while $\mu = 0.2$ is that determined in reference 12. Both values of τ_0 are in good agreement with the result of Goettler and Faber for the same nominal composition matrix.

For the SiC/borosilicate glass system, the push-out test shows either one or two plateaus (Figure 9). As described above, based on the debond strength of SiC/glass, loads < 140 g should exhibit a single plateau while those > 140 g should exhibit two plateaus. The first case is shown in Figure 9a. The force at the plateau gives a value of τ_d of 38 MPa for the core slipping through the SiC. The second case is shown in Figure 9b, where the force at the first plateau gives a value of τ of 36 MPa for the core slipping in SiC and the force at the second plateau gives a value of τ of 10 MPa for the SiC slipping in the matrix. Tests on additional fibers gave an average value of τ of 30 ± 9 MPa for the core in SiC. The value of τ for SiC in the matrix is in reasonable agreement with τ_d obtained from the single fiber pull-out test. These results are based on a fairly small number of fibers and additional

verification is required to more firmly establish these values. In addition to more data, precise measurements of the indentations need to be made and Marshall's analysis applied to the data to confirm that the two methods agree.

Examination of the SiC/glass-ceramic system shows that τ is dependent on the investigator as well as the technique. The indentation push-in results yield τ 's varying from 1 to 10 MPa, depending on the investigator [6,13,16,17] and from 1 to 100 MPa, depending on the heat treatment [16]. The discrepancy in heat treated materials is due to differences in the fiber-matrix interface bonding with some fibers being more tightly bound than others. This would lead to differences in both debond strength and frictional pull-out. The discrepancy in various untreated materials is due to both differences in the fiber-matrix bond and fiber misorientation with respect to the applied force.

In a sample which is 2 mm in thickness, the indentation test was either of the push-in or push-out type. Typical results are shown in Figures 2 and 10. In Figure 2, a push-in type is shown while Figure 10 shows a push-out result. In both cases, however, τ is on the order of 1-6 MPa for this system, leading to the conclusion that this τ is due to frictional effects. Values of τ as high as 55 MPa were also observed, leading to the supposition that there are differences in the bonding between fiber and matrix at different locations in the specimen. The indentation push-out test results are more difficult to obtain because of the need to use flat and polished samples. Based on a number of measurements, however, the indentation push-out results are more reproducible than are the indentation push-in results. For this thickness sample, it is apparent that the assumptions for both types of test are met. For thinner samples, the assumption that the thickness \gg fiber diameter may be violated, thus τ_f determined from the plateau region of the push-out test may not agree with that obtained in the initial region where push-in is

assumed to take place. The analysis of the push-out test in the plateau region is simpler than that required for the push-in test and is not affected by the assumptions regarding elastic interactions after the force is released and what happens below the slip region during testing.

SUMMARY

For soda-lime-silica glass/SiC monofilament, interfacial frictional stresses of around 14 MPa, debond strengths of about 19 MPa, and coefficients of friction between 0.03 and 0.17 were obtained. These values may be significantly affected by the glass/fiber/air surface stress discontinuity. For the calcia-titania-silica glass/SiC monofilament, interfacial frictional stresses and debond strengths were both on the order of 3 MPa.

Compared to borosilicate glass system, the frictional stresses in the soda-lime-silica system are higher due to the higher normal compressive stress at the fiber-matrix interface. These higher stresses are the result of the larger difference in thermal expansion coefficients between the soda-lime-silica glass and SiC fiber than between the borosilicate glass and SiC fiber. The calcia-titania-silica system has a frictional stress about the same as that observed in borosilicate glass, but shows a significantly lower debond strength. At this point, the supposition is that chemical bonding effects in the calcia-titania-silica system dominate the pull-out process, even though debonding of the fiber from the matrix due to the smaller thermal expansion coefficient of the glass than the fiber would be expected to strongly influence the behavior. This apparent anomaly is being explored further before any additional conclusions can be drawn.

The low friction coefficients obtained in the soda-lime-silica system suggest the presence of a lubricating layer between the fiber and the matrix,

perhaps due to processing. At this time, there are no plans to further investigate this behavior.

The single fiber pull-out test provides the most direct method of determining the interfacial strengths, both debonding and frictional, but at present can only be used effectively for large fiber diameters, primarily due to specimen handling considerations. The indentation tests use a minimal amount of material and can be performed on samples containing either large monofilaments or small diameter multifilament tows but provide information on only τ_f (push-in) or τ_f or τ_d (push-out), depending on indenter geometry and material characteristics. It is possible that the push-out test can be performed at slower loading rates and with a different indenter geometry, thus allowing for separation of the debonding strength from the interfacial friction stress in the force²-displacement curve. The preparation of indentation push-out samples is more difficult than for indentation push-in samples but the analysis is simpler and the results appear to be more reproducible. While there are some discrepancies yet to be resolved, interfacial strengths determined using different test methods agree well with one another as do debond strengths determined using different methods. Based on the ability to measure both debond strength and interfacial frictional stress, and the need to use a minimal amount of material, the indentation push-out test appears to be the most desirable one to use.

FUTURE PLANS

During the coming year, we will focus on two areas: coatings for interface control and high temperature mechanical testing. There are two key issues involved in the selection of fiber coatings. The first is the effect of the coating on both the interfacial bond between the fiber and the matrix

as well as the frictional stress needed to draw the fiber from the matrix once the initial bond is broken. There is clearly an optimum value needed for both parameters in order to achieve high strength as well as damage tolerance. The second issue involves the stability of the fiber/matrix interface at elevated temperatures. The coatings will be characterized using standard electron and optical microscopy techniques as well as via scanning Auger and other appropriate surface analytical techniques. The fiber/matrix interfaces will be characterized using the single fiber pull-out test as well as instrumented indenter techniques, both before and after exposure to high temperatures.

To the extent that experimental data is or can be made available, comparison of the predictions for microcracking stresses using the information from the single fiber tests will be made with tensile test data on composites of these materials. Efforts will be initiated to resolve any discrepancies which are noticed.

REFERENCES

1. J. Aveston, G. A. Cooper, and A. Kelly, The Properties of Fibre Composites, National Physical Laboratory, Science and Technology Press Ltd., London, 1971, pp. 15-26.
2. J. Aveston and A. Kelly, *J. Mat. Sci.*, 8 352 (1973).
3. D. B. Marshall and A. G. Evans, *J. Amer. Ceram. Soc.*, 68 225 (1985).
4. D. B. Marshall, B. N. Cox, and A. G. Evans, *Acta Metall.*, 33 2013 (1985).
5. B. Budiansky, J. W. Hutchinson, and A. G. Evans, *J. Mech. Phys. Solids*, 34 167 (1986).
6. D. B. Marshall, *J. Amer. Ceram. Soc.*, 67 C259 (1985).
7. B. Harris, J. Morley, and D. C. Philips, *J. Mat. Sci.*, 10 2050 (1975).
8. M. R. Piggott, A. Sanadi, P. S. Chua, and D. Andison in Composite Interfaces, H. Ishida and J. L. Koenig, eds., Elsevier, 1986, p. 109.

9. L. S. Penn and S. M. Lee, *Fibre Sci. Tech.*, 17 19 (1982).
10. U. V. Deshmukh and T. W. Coyle, *Cer. Eng. Sci. Proc.*, 9 627 (1988).
11. C. W. Griffin, S. Y. Limaye, D. W. Richerson, and D. K. Shetty, *Cer. Eng. Sci. Proc.*, 9 671 (1988).
12. R. W. Goettler and K. T. Faber, *Cer. Eng. Sci. Proc.*, 9 861 (1988).
13. D. B. Marshall and W. C. Oliver, *J. Amer. Cer. Soc.*, 70 [8] 542 (1987).
14. R. A. Lowden, Oak Ridge National Laboratory, private communication, 1988.
15. J. F. Mandell, D. H. Grande, T.-H. Tsiang, and F. J. McGarry in Composite Materials: Testing and Design, ASTM STP 893, J. M. Whitney, ed., ASTM, Philadelphia, 1986, pp. 87-108.
16. T. W. Coyle, H. M. Chan, and U. V. Deshmukh in Interfaces in Polymer, Ceramic, and Metal Matrix Composites, H. Ishida, ed., Elsevier, Amsterdam, 1988, pp. 489-501.
17. U. V. Deshmukh, A. Kanei, S. W. Freiman, and D. C. Cranmer in High Temperature/High Performance Composites, MRS Symposium Volume 120, Materials Research Society, 1988, pp. 253-258.

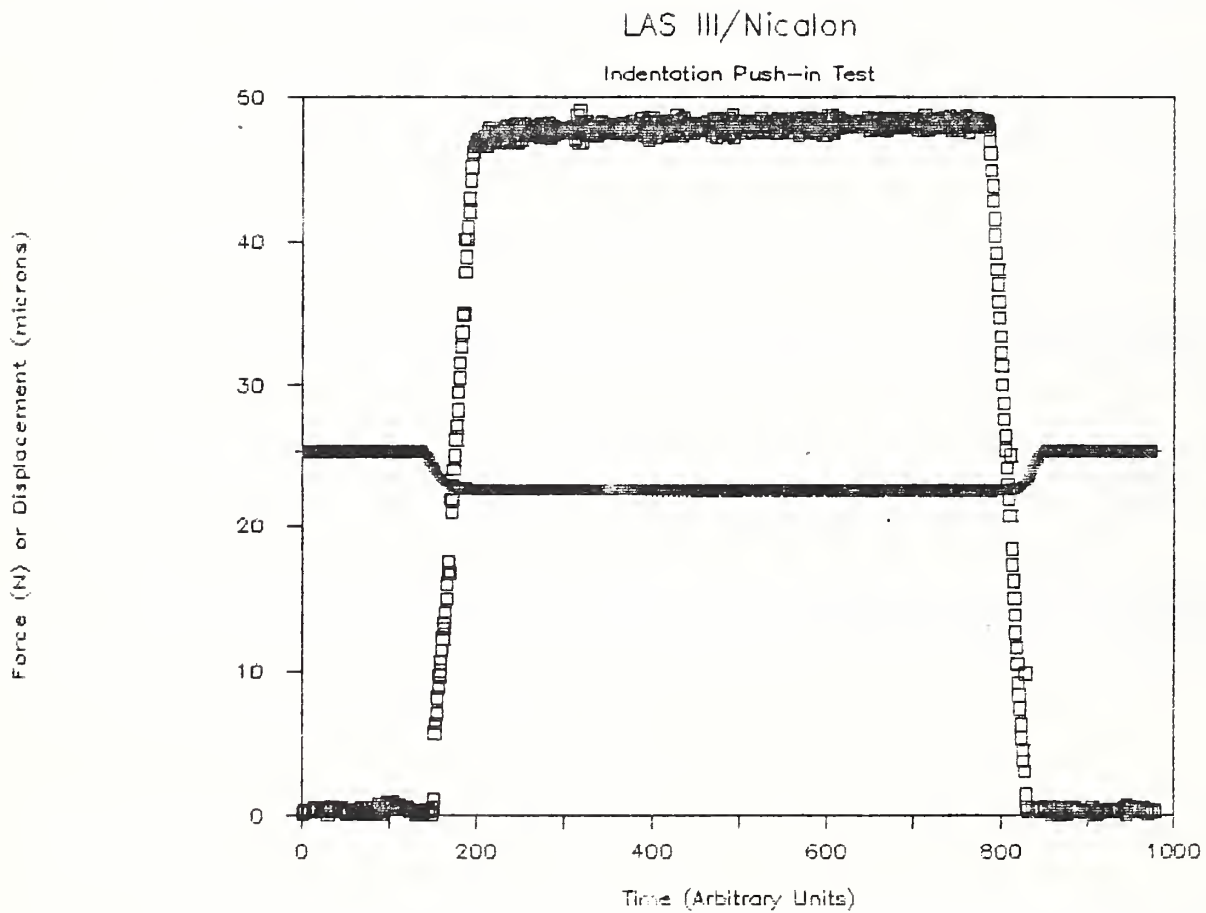


Figure 1. Typical results of load and displacement versus time for instrumented indenter testing of ceramic composites.

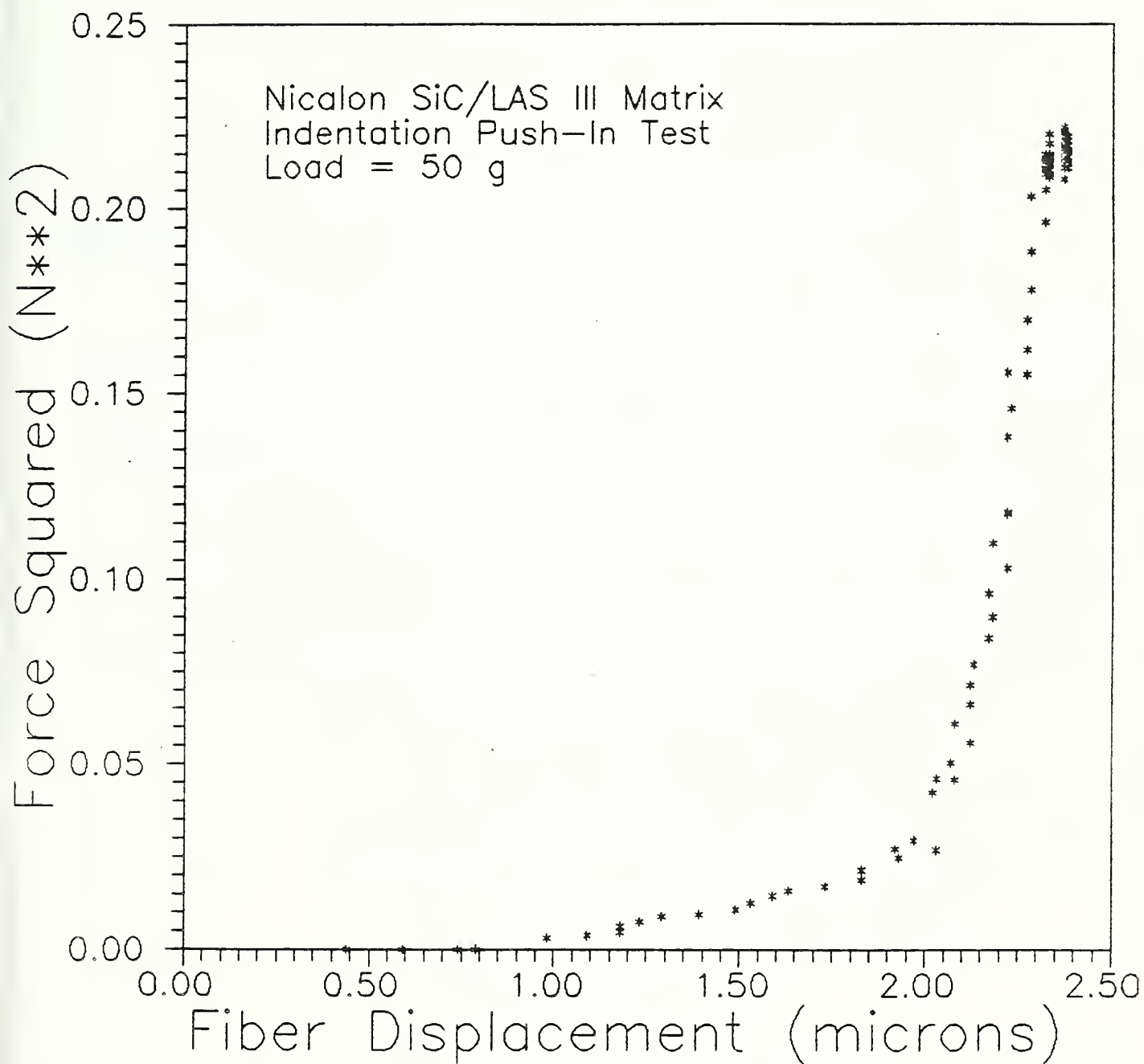


Figure 2. Typical force squared (F^2) versus displacement (δ) for indentation push-in test. Material is LAS III matrix/Nicalon fiber.

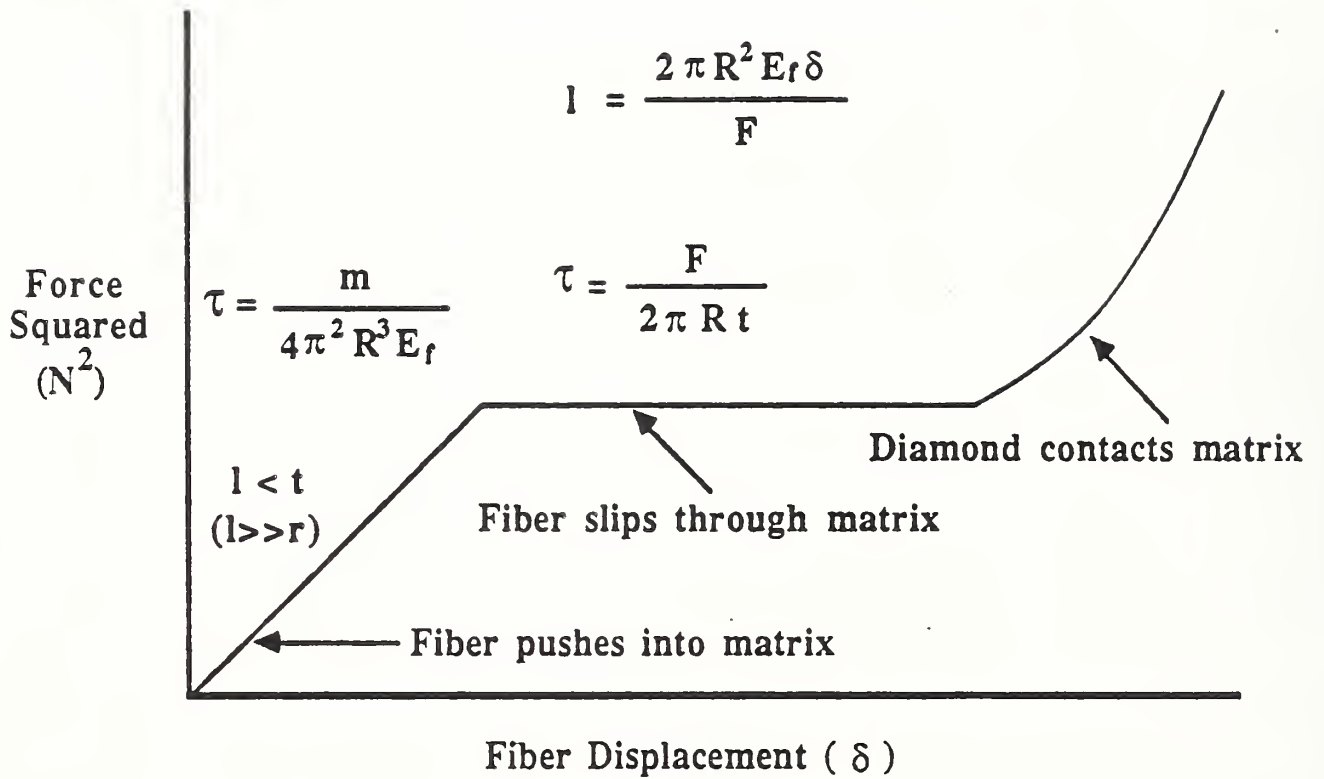


Figure 3. Schematic of F^2 versus δ for indentation push-out test.

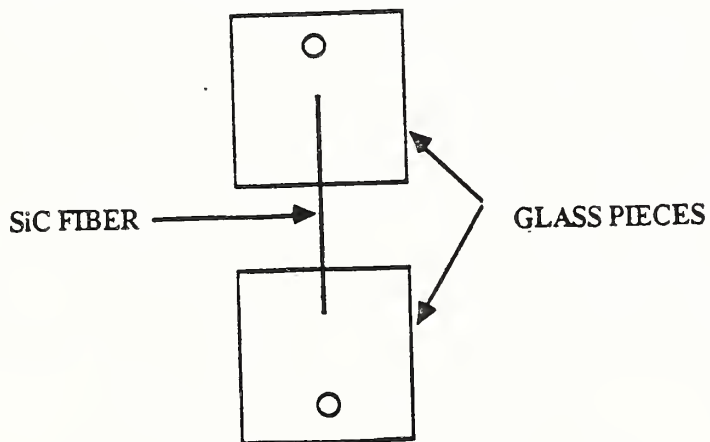
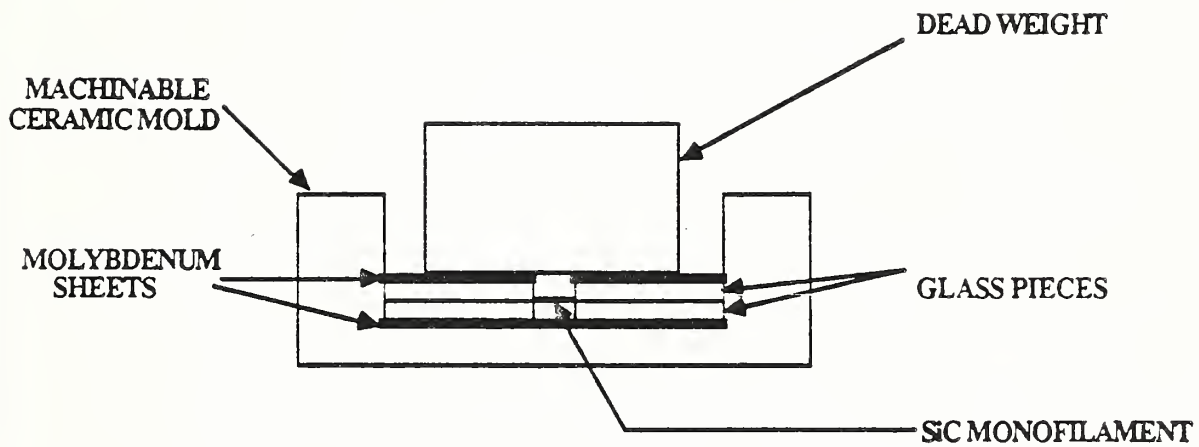


Figure 4. Schematic of sample making assembly and finished sample.

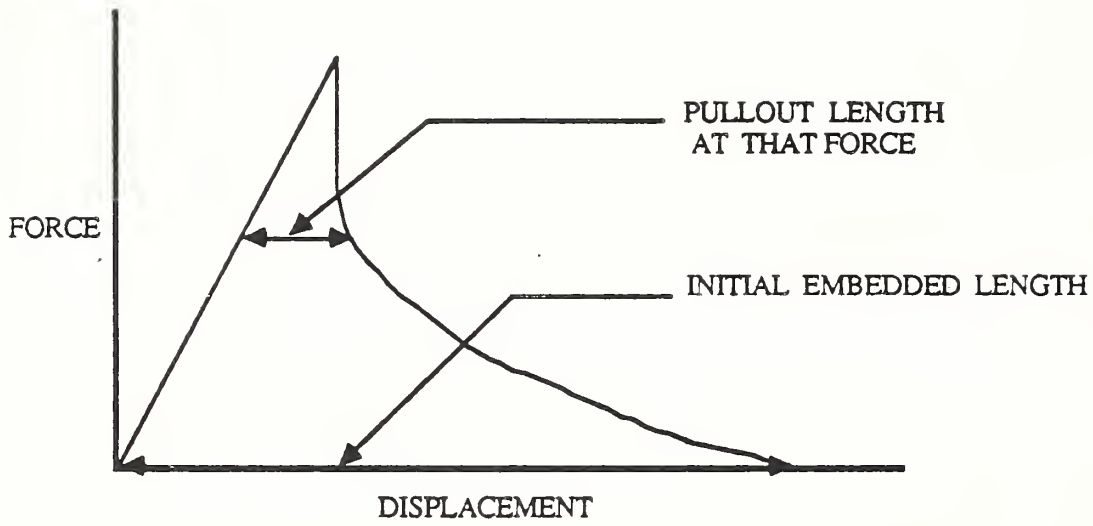


Figure 5. Measurement of pull-out and initial embedded length from a force-displacement curve.

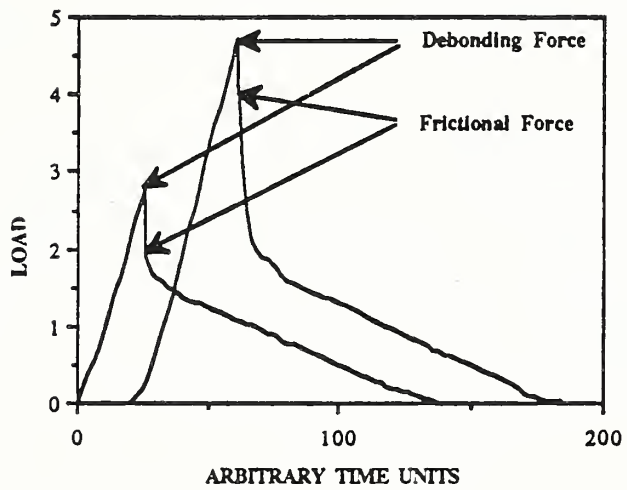


Figure 6. Typical force-displacement curves observed in soda-lime-silica/SiC system.

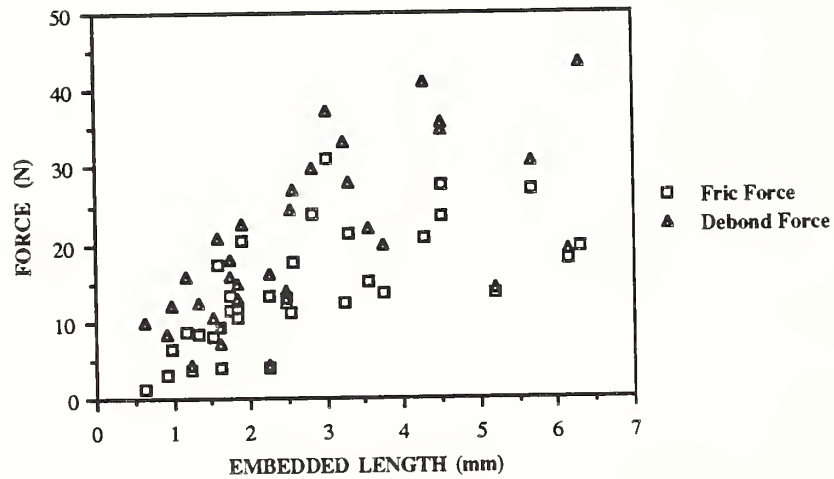


Figure 7. Plot of maximum pull-out force versus embedded length for soda-lime-silica/SiC system. Debond force is based on the maximum load observed during the test; frictional force is based on a lower load for which only frictional forces are operating on the interface.

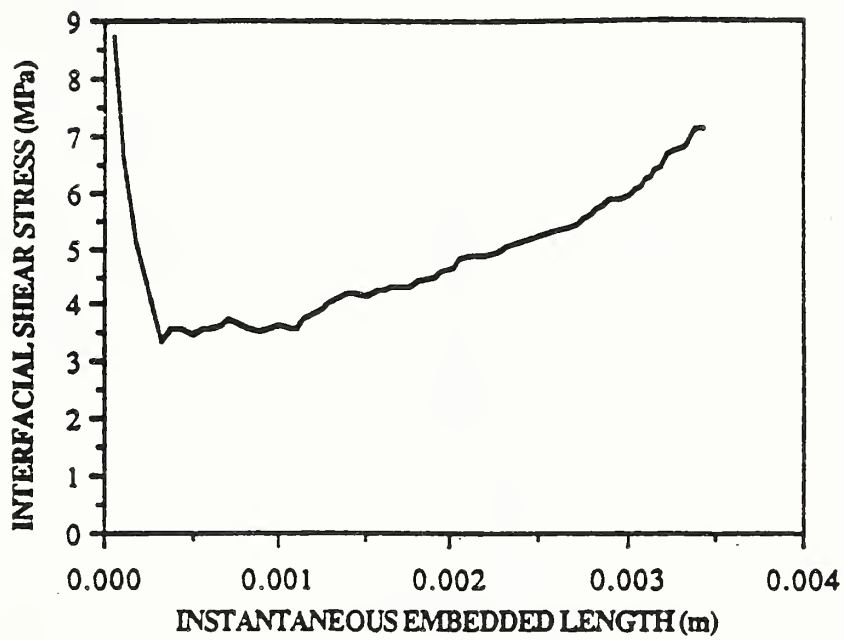


Figure 8. Stability of frictional stress during pull-out test.

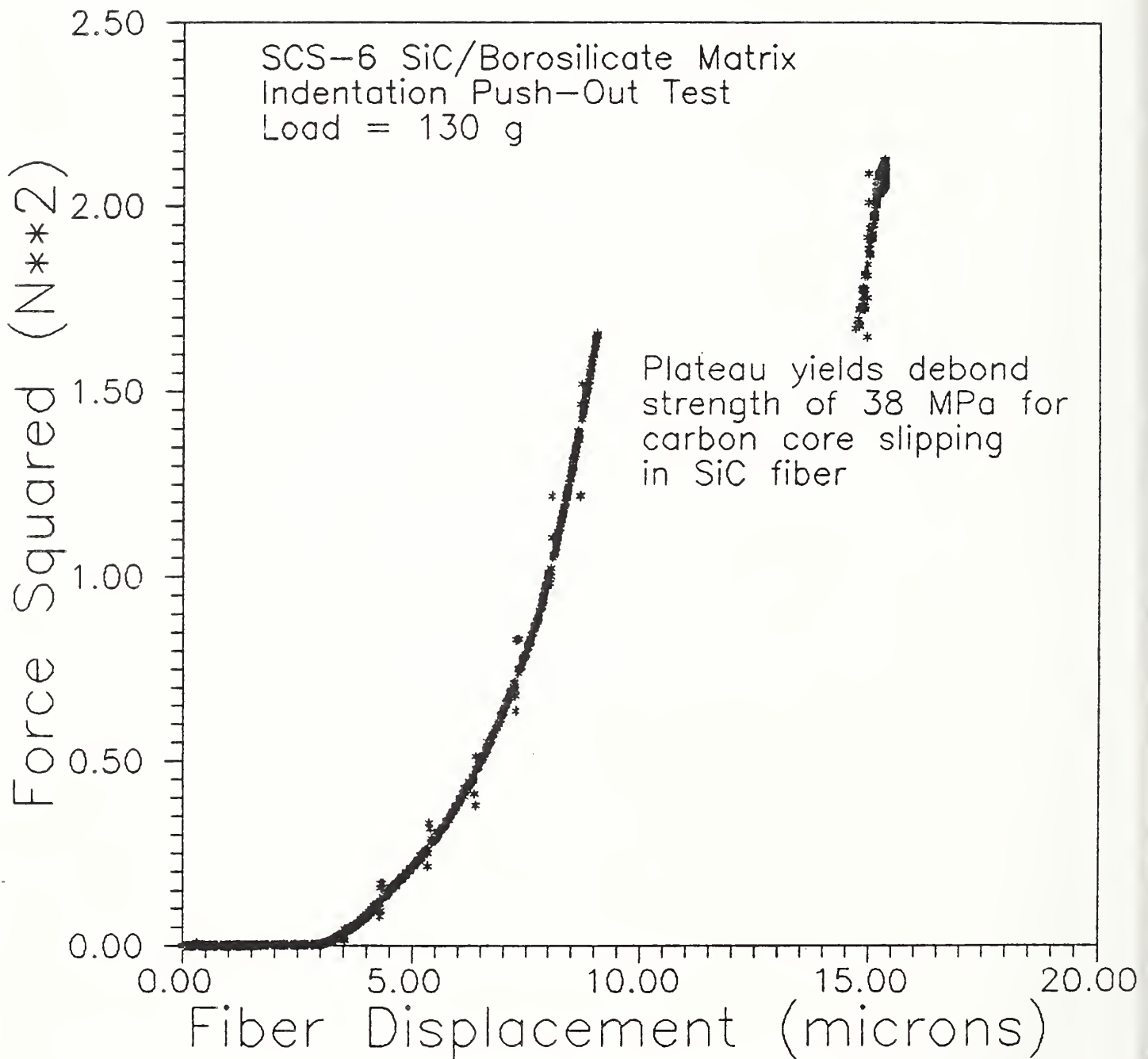


Figure 9. Results of indentation of SiC monofilament in borosilicate glass matrix.
 a. Indentation load = 130 grams.

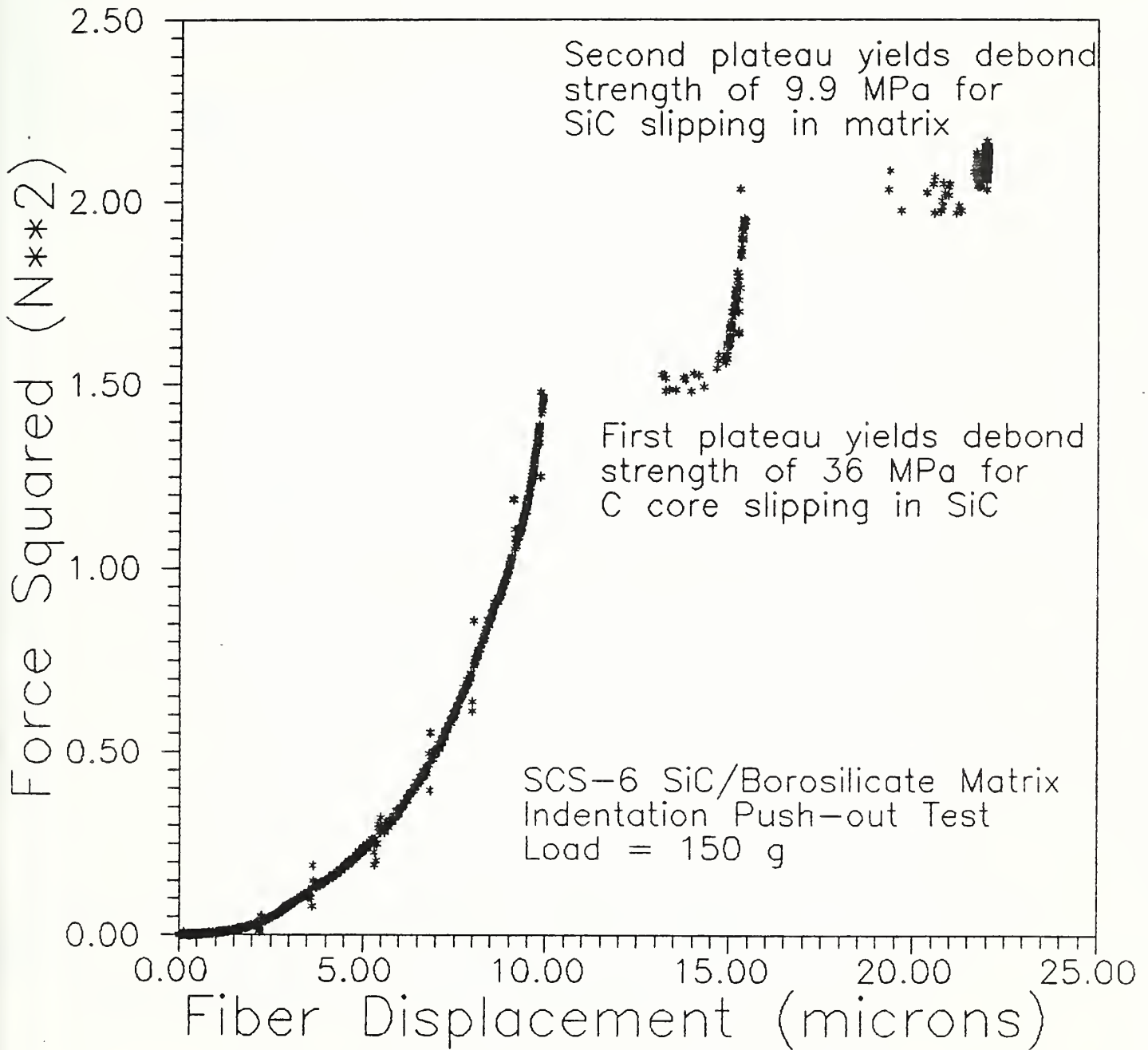


Figure 9. Results of indentation of SiC monofilament in borosilicate glass matrix.

b. Indentation load = 150 grams.

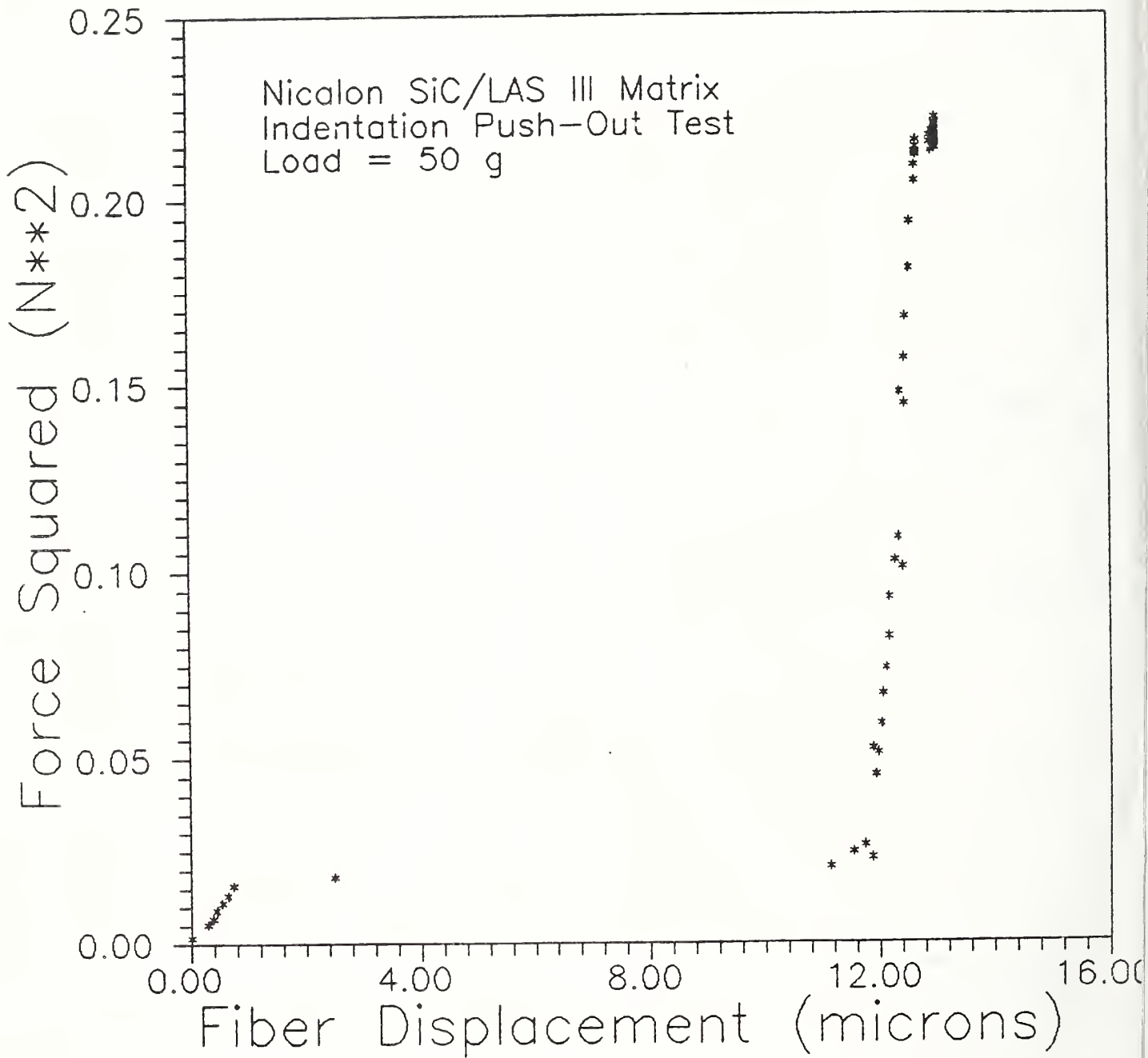


Figure 10. Results of indentation push-out test ($l > t$) of SiC in LAS III matrix.

EFFECT OF THERMAL EXPANSION MISMATCH ON FIBER PULL-OUT IN GLASS MATRIX COMPOSITES

U. V. Deshmukh*, A. Kanei*, S. W. Freiman** and D. C. Granmer**

*Department of Materials Engineering, Drexel University, Philadelphia, PA 19104

**Ceramics Division, National Bureau of Standards, Gaithersburg, MD 20899

ABSTRACT

Single fiber pull-out tests can be used to directly measure the fiber-matrix interfacial shear stress in glass matrix composites. The system under investigation consisted of a soda-lime-silica glass matrix containing SiC monofilaments with a carbon-rich surface. The presence of the carbon-rich layer on the surface of these fibers makes them non-wetting to most glasses; hence the fibers are held in the matrix only by frictional forces acting at the interface. The mechanical gripping responsible for this force can be changed by manipulating the glass matrix/fiber thermal expansion coefficient mismatch. Frictional stresses (τ) and friction coefficients (μ) obtained for SiC monofilaments in a soda-lime-silica glass matrix were compared with previously obtained data on a borosilicate glass matrix ($\tau = 2-3$ MPa, $\mu = 0.72 \pm 0.36$). For the soda-lime-silica system, τ 's of 4-20 MPa and μ of 0.10 ± 0.03 were obtained. τ in the soda-lime-silica system is higher due to the larger difference in thermal expansion mismatch between the fiber and matrix. The differences in μ may be due to lubrication effects caused by water at the fiber-matrix interface.

INTRODUCTION

Strengths of fiber-matrix interfaces have been measured by several different techniques, but single fiber pull-out tests give the most direct measure of the interface strength [1-3]. Depending on the nature of the interaction (chemical and/or mechanical) between the fiber and the matrix, a single fiber pull-out test gives information about both the debonding and pull-out processes occurring in composites. However, single fiber pull-out tests have been used for glass matrix systems only recently [4-6].

The stress analysis of the test is based on the shear-lag theory of Cox [7], as modified by Greszczuk [8] and Lawrence [9] for elastically loaded brittle matrices. A good review of recent developments in this area is given by Gray [10]. In the absence of a chemical bond across the interface, or if an existing bond is broken, the resistance to fiber pull-out is mainly from interfacial frictional stresses, τ . If the matrix shrinks more than the fiber (due to thermal expansion), a residual compressive stress acting at the interface is produced, which depends on the elastic properties of the fiber and matrix, the difference in thermal expansion between the fiber and matrix, and the temperature difference between the glass strain point (T_s) and room temperature (T_{rt}). When $\alpha_{\text{glass}} > \alpha_{\text{SiC}}$, a larger thermal expansion coefficient difference should lead to a larger compressive stress, and thus to a higher resistance to pull-out. To confirm this hypothesis, experimental data were collected on a soda-lime-silica glass/SiC fiber system for comparison with data [4] on a borosilicate glass/SiC fiber system.

BACKGROUND

In a previous study [4] of a borosilicate glass/SiC monofilament system, a simple model was used where τ was estimated as the maximum pull-out force divided by the contact area. The contact area was taken to be $2\pi rL$, where r is the fiber radius and L is the initial embedded length. This value of τ is probably related to the debonding of the fiber from the matrix. This model is inaccurate since it does not account for Poisson contraction of the fiber radius as a result of the tensile pull-out force nor does it account for shear

stresses occurring where the fiber emerges from between the glass plates. This latter effect is assumed to be a fixed quantity which cannot yet be accounted for. In the present paper, we have used the model of Takaku and Arridge [11], which takes into account the effect of Poisson's contraction. Their expression for the axial stress acting on the fiber is:

$$\sigma_f = \sigma_0/k [1 - \exp(-2\mu kL/\tau)] \quad (1)$$

where σ_0 is the normal compressive stress acting at the interface in the unstressed material, k is a constant determined by the elastic properties of the fiber and matrix [$= E_m \nu_f / E_f (1 + \nu_m)$; E is Young's modulus, ν is Poisson's ratio], and μ is the friction coefficient. By measuring σ_f as a function of embedded length, in principle we can obtain values for σ_0 and μ . As demonstrated in reference 4, however, due to scatter in the data for σ_f , a reliable value for σ_0 could not be obtained in this way. We therefore determined σ_0 using the expression of Vedula et. al. [12] for the residual stress developed in a composite due to anisotropic thermal expansion of fiber and matrix:

$$\sigma_0 \cong \sigma_{r,f} = (\sigma_1 \Delta\alpha_l + \sigma_2 \Delta\alpha_r) \Delta T \quad (2)$$

where σ_1 and σ_2 are constants, $\Delta\alpha_l$ and $\Delta\alpha_r$ are the differences in thermal expansion coefficients between the fiber and matrix in the longitudinal and radial directions, respectively, and ΔT is the cooling range viz. $T_{r1} - T_0$.

EXPERIMENTAL PROCEDURE

Soda-lime-silica glass has a thermal expansion coefficient of $82 \times 10^{-7}/^\circ\text{C}$ compared to $32 \times 10^{-7}/^\circ\text{C}$ for borosilicate glass. The SiC monofilament longitudinal expansion is $26 \times 10^{-7}/^\circ\text{C}$, while the radial expansion is $25.3 \times 10^{-7}/^\circ\text{C}$ [6]. Samples were fabricated by sandwiching SiC monofilaments* between soda-lime-silica glass plates* and heating under dead weight loading corresponding to 14-21 KPa pressure as shown in Figure 1. Molybdenum sheets were placed between the dead weight and the glass plates to prevent adhesion during fabrication. The entire assembly was immersed in graphite powder to prevent oxidation of the fibers. Industrial grade argon was kept flowing through the furnace. The samples were held at temperature ($725-760^\circ\text{C}$) for different times (30-90 min) to obtain good flow of the glass around the monofilament. A schematic of the finished samples is shown in Figure 1. Different embedded lengths were obtained by varying the length of the monofilament between the plates. Individual samples were loaded in uniaxial tension on a universal test machine[†]. The samples were gripped using swivel hooks attached to ball joints to facilitate alignment of the fiber with the stress axis. Samples were pulled at a rate of 0.05 cm/min. The embedded length was determined from the force-displacement curves (Figure 2) since accurate optical measurements could not be made due to uncertainty in where the monofilament emerged from between the glass plates.

* SCS-6 SiC monofilaments, AVCO Corp., Lowell, MA. Trade names and companies are identified in order to adequately specify the materials used. In no case does such identification imply that the products are necessarily the best available for the purpose.

[†] Fisher Brand, Fisher Scientific, Pittsburgh, PA.

[‡] Instron Corp., Canton, MA.

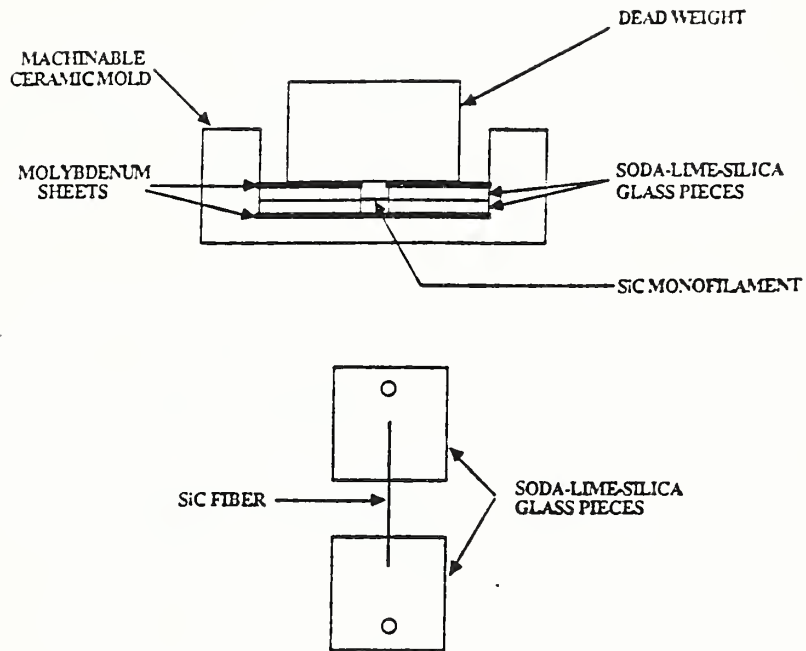


Figure 1. Schematic of the sample-making mold assembly and individual sample.

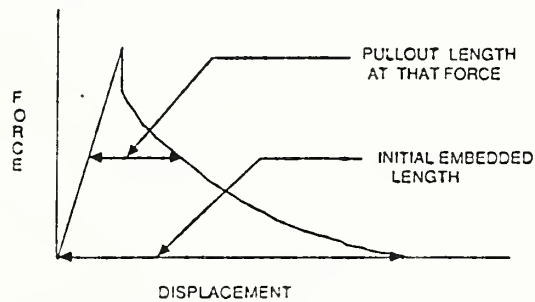


Figure 2. Measurement of pull-out and initial embedded length from a force-displacement curve.

RESULTS AND DISCUSSION

Two types of force-displacement curve were observed in the soda-lime-silica glass/SiC fiber system as shown in Figure 3. In both cases, the load increased linearly with displacement until the fiber debonded from the matrix. In the first case, there was a sharp drop in load, followed by pull-out of the fiber. In the second case, the load decreased gradually from the maximum while the fiber pulled out. The incidence of "stick-slip" behavior during pull-out was much less frequent than in the borosilicate glass/SiC system [4], suggesting the presence of a lubricating layer between the fiber and the soda-lime-silica matrix.

The maximum force required to initiate pull-out of the fiber is plotted vs embedded length in Figure 4. Although there is considerable scatter in the data, it can be seen that the pull-out force increases with increasing embedded length as long as the fiber strength is not exceeded. Some of the scatter may be due to non-uniform flow of glass around the fiber, leading to an air gap at the interface, and therefore reduced contact area and pull-out force. Also plotted in Figure 4 are the loads at which only frictional forces are acting on the interface. The difference between the maximum load and the frictional load is not constant. To confirm that the first load drop is due to debonding, several samples were unloaded following the initial load drop, then reloaded. Upon reloading, pull-out was observed at the same load where unloading had occurred, showing that the fiber-matrix bonds were in fact broken initially and that only frictional stress was operating at the interface. Occasionally, after reloading, a very small load drop was observed which is attributable to the difference between the static and dynamic coefficients of friction. The stability of τ during pull-out over a wide range of instantaneous embedded length is demonstrated in Figure 5.

Table 1 shows τ calculated from Equation 1 for both the soda-lime-silica and borosilicate glass systems. The large standard deviation for the soda-lime-silica system is believed to be due to variations in processing conditions. After making appropriate substitutions in Equation 2 for $\Delta\alpha_p$, $\Delta\alpha_r$, ΔT , σ_1 , and σ_2 (see Table 1), the frictional stress, σ_0 , for the soda-lime-silica/SiC system is estimated to be about 150 MPa. Similar calculations for borosilicate glass/SiC give a value for σ_0 of about 16 MPa. By substituting values for σ_0 in Equation 1, the friction coefficient, μ , can be obtained. For the soda-lime-silica system, μ was calculated to be 0.10 ± 0.03 ; for the borosilicate system, μ is 0.72 ± 0.36 . The frictional stress acting at the interface may now be calculated as the product of μ and σ_n , where $\sigma_n = \sigma_0 - k\sigma_r$, σ_r being the axial stress corresponding to the frictional force and $k\sigma_r$ representing the reduction in σ_n due to Poisson's contraction. For the soda-lime-silica system, τ was calculated to range from 4-20 MPa while for the borosilicate system, it was in the range from 2-3 MPa.

SUMMARY

- (1) Single fiber pull-out tests were used successfully to evaluate the frictional shear stress in glass matrix composites.
- (2) For soda-lime-silica glass/SiC monofilament, τ of 4-20 MPa and μ of 0.10 ± 0.03 were obtained. These values may be significantly affected by the glass/fiber/air surface stress discontinuity.
- (3) Compared to borosilicate glass system, the frictional stresses in the soda-lime-silica system are higher due to the higher normal compressive stress at the fiber-matrix interface. These higher stresses are the result of the larger difference in thermal expansion coefficients between the soda-lime-silica glass and SiC fiber than between the borosilicate glass and SiC fiber.

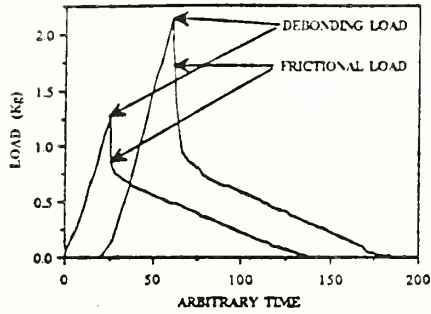


Figure 3. Typical force-time curves observed in soda-lime-silica/SCS-6 system.

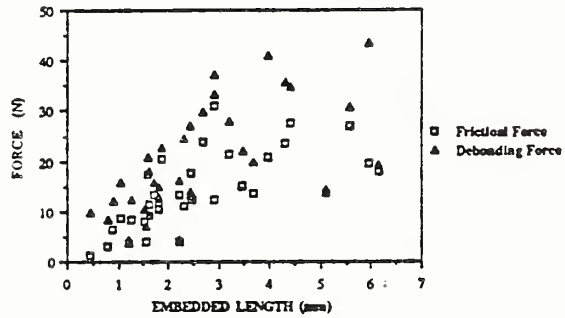


Figure 4. Plot of maximum pull-out force vs embedded length for soda-lime-silica glass/SiC monofilament. Debond force is based on the maximum load observed during the test; frictional force is based on a lower load for which only frictional forces are operating on the interface.

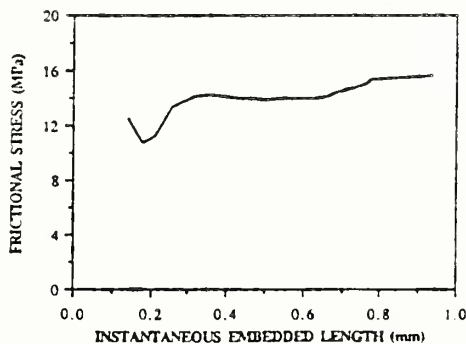


Figure 5. Plot of frictional stress throughout a single pull-out test as a function of instantaneous embedded length.

Table 1
Frictional Shear Stress and Friction Coefficients
Calculated from Equation 1
(Numbers in parenthesis represent number of samples averaged)

<u>Matrix Material</u>	<u>Borosilicate Glass</u>	<u>Soda-Lime-Silica Glass</u>
$\Delta\alpha_f$ ($\times 10^6/^{\circ}\text{C}$)	0.6	5.6
$\Delta\alpha_m$ ($\times 10^6/^{\circ}\text{C}$)	0.67	5.67
ΔT ($^{\circ}\text{C}$)	495	440
σ_1 (GPa)	6.6	7.5
σ_2 (GPa)	47.0	52.7
σ_0 (MPa)	16.2	153.8
μ	0.72 ± 0.36 (9)	0.10 ± 0.03 (27)
τ (MPa)	3.6 ± 0.7 (9)	13.9 ± 4.1 (27)

(4) The low friction coefficients obtained in the soda-lime-silica system suggest the presence of a lubricating layer between the fiber and the matrix, perhaps due to processing.

ACKNOWLEDGEMENTS

The authors would like to thank Profs. M. J. Koczak and M. Barsoum for helpful discussions. We are grateful to Dr. S. G. Fishman for support through SDIO/IST contract N00014-86-F-0096.

REFERENCES

- 1) B. Harris, J. Morley, and D. C. Philips, *J. Mat. Sci.*, 10 2050 (1975).
- 2) M. R. Piggott, A. Sanadi, P. S. Chua, and D. Andison in Composite Interfaces, H. Ishida and J. L. Koenig, Elsevier, 1986, p. 109.
- 3) L. S. Penn and S. M. Lee, *Fibre Sci. Tech.*, 17 19 (1982).
- 4) U. V. Deshmukh and T. W. Coyle, to be published in *Cer. Eng. Sci. Proc.*
- 5) C. W. Griffin, S. Y. Limaye, D. W. Richerson, and D. K. Shetty, *ibid.*
- 6) R. W. Goettler and K. T. Faber, *ibid.*
- 7) H. L. Cox, *Brit. J. Appl. Phys.*, 3 72 (1952).
- 8) L. B. Greszczuk in Interfaces in Composites, ASTM STP 452, 1969, p. 43.
- 9) P. Lawrence, *J. Mat. Sci.*, 7 1 (1972).
- 10) R. J. Gray, *J. Mat. Sci.*, 19 861 (1984).
- 11) A. Takaku and R. G. C. Arridge, *J. Phys. D*, 6 2038 (1973).
- 12) H. Vedula, R. N. Pangborn, and R. A. Queeney, *Composites*, 19 55 (1988).

COMPARISON OF METHODS FOR DETERMINING FIBER/MATRIX INTERFACE FRICTIONAL
STRESSES IN CERAMIC MATRIX COMPOSITES

David C. Cranmer*, Uday V. Deshmukh[†], and Thomas W. Coyle[#]

*National Institute of Standards and Technology, Gaithersburg, MD 20899

[†]Dept. of Materials Engineering, Drexel University, Philadelphia, PA 19104

[#]Ecole Nationale Supérieure de Mécanique, Nantes Cedex, FRANCE

ABSTRACT: In this study, several experimental methods including indentation push-in, indentation push-out, and single fiber pull-out tests were employed to measure the strength of the fiber/matrix bond in two continuous fiber reinforced ceramic matrix composites. The composite systems examined were a SiC monofilament reinforced borosilicate glass matrix and a SiC fiber tow reinforced glass-ceramic matrix. Single fiber pull-out test results gave debond strengths (τ_d) of 11.1 ± 3.2 MPa and interface frictional stresses (τ_f) of 3.6 ± 0.7 MPa for the SiC/borosilicate system. In the push-out test, τ_d for the SiC/borosilicate system appears to be about 10 MPa while τ 's between 1 and 55 MPa were obtained in the SiC/glass-ceramic composite. The push-in test gave values of τ_f between 2 and 34 MPa for the SiC/glass-ceramic system. Variability in τ within a specimen is due to differences in bonding between the fibers and matrix at various locations. The discrepancies in τ both within a test and between test methods are explained in terms of fiber/matrix bonding and test geometry. The most versatile test method appears to be the indentation push-out test.

Key Words: glass-ceramic composites, glass composites, mechanical properties, fiber/matrix interfacial strength, indentation push-in, indentation push-out, fiber pull-out

INTRODUCTION

The strength of the fiber-matrix interface is one of the key parameters responsible for the stress-strain behavior and damage tolerance of ceramic composites. These interfacial strengths (τ) have been measured by several different techniques [1-6] including indentation push-in, indentation push-out, and single fiber pull-out. The interfacial strength which can be measured is one of two types: debond (τ_d) and frictional (τ_f). The debond strength is related to the degree of chemical bonding between the fiber and the matrix, while the frictional stress relates to the slippage of the fiber in the matrix. The purpose of this paper is to compare these methods for obtaining τ_d and τ_f , both in terms of the ease of use and the consistency and reproducibility of the numbers obtained from each technique.

As will be shown in more detail in the Background Section, no one material lends itself to testing using all three methods, and no single test method provides all of the information desired on interfacial mechanical properties. The reasons for this are as follows. In a single fiber pull-out test, the combination of a small fiber diameter (10-20 μm) for materials such as Nicalon SiC¹, high temperature (>700°C) processing required to obtain an acceptable sample geometry, and handling to set up each experiment makes it difficult at best to perform the test on a large enough number of samples. In the indentation push-in test, the large monofilaments tend to crush rather than slide, thus obliterating the indentation impressions and yielding inaccurate displacement measurements. To date, no work has been published regarding the use of the indentation push-out test on layered fibers such as

¹ Nicalon SiC, Nippon Carbon Co., Ltd., Tokyo, Japan. Trade names and companies are identified in order to adequately specify the materials and equipment used. In no case does such identification imply that the products are necessarily the best available for the purpose.

SiC deposited on C or W cores. In view of these problems, two model composite systems were chosen which were amenable to measurements by more than one technique. The model systems examined include a borosilicate glass matrix reinforced by SiC monofilaments² and a lithium aluminosilicate glass-ceramic matrix reinforced by SiC fibers³. The borosilicate glass system was tested using the pull-out and indentation push-out techniques, while the glass-ceramic system was tested using the two indentation techniques.

BACKGROUND

Single Fiber Pull-out

Single fiber pull-out tests give the most direct measure of the interface strength [6-11], but the tests performed to date have only been conducted on monofilaments. Depending on the nature of the interaction (chemical and/or mechanical) between the fiber and the matrix, the single fiber pull-out test gives information about both the debonding and frictional processes occurring in composites. However, single fiber pull-out tests have been used for glass matrix systems only recently [6,10,11].

In a previous study [10] of a SiC/borosilicate glass monofilament system, τ_f was determined as 5 - 6.5 MPa. A simple model based on a shear-lag analysis was used where τ was estimated as the pull-out force divided by the contact area. This model is inaccurate since it does not account for differential Poisson contractions of the fiber and matrix as a result of the tensile pull-out force nor does it account for surface stress concentrations occurring where the fiber emerges from between the glass plates. In a

² SCS-6, Textron Specialty Materials, Lowell, MA.

³ Nicalon SiC/LAS-III, United Technologies Research Center, East Hartford, CT.

subsequent paper [5], Poisson contraction was taken into account, and τ_f was determined to be on the order of 3.5 MPa, a decrease of 30-45% compared to that calculated using the simple analysis. In this same paper, τ_d was determined to be 11 MPa.

An alternate analysis [6], also based on the shear lag theory, yields τ_f 's between 15 and 30 MPa, depending on the exact glass composition. This analysis assumes the presence of a residual stress in the fiber due to thermal expansion mismatch between the fiber and the matrix. Evaluation of the interfacial frictional stress is thus broken into two components: one a residual stress-free bonding term (τ_0), the other the contribution due to residual stresses ($\mu\sigma_{rm}$). τ_0 should vary with fiber surface chemistry, while $\mu\sigma_{rm}$ should vary with processing conditions, sample geometry, and matrix composition. The values of τ_f obtained in reference 6 are significantly higher than obtained using the previous analyses. At present, there is insufficient basis, either experimental or theoretical, on which to choose one model over the other.

Indentation Tests

Indentation testing to determine τ_f was first initiated by Marshall [1]. Fiber/matrix frictional stresses of 2.5 ± 0.9 MPa were measured for a SiC-reinforced glass-ceramic², but the method requires precise measurement of very small indentation sizes, potentially a significant source of error. The analysis assumes that the elastic depression of the matrix adjacent to the indented fiber, the stress field of the indent and the surface stress concentrations, as well as changes in fiber diameter due to Poisson's expansion can be neglected. For the analysis to be valid, the specimen thickness must be large compared to the diameter of the fiber. The analysis

also does not account for non-orthogonal loading of the fiber or misorientation of the fiber from a direction parallel to the applied force. Additional studies by Marshall and Oliver [3] refined the method by using a pyramidal indenter at ultralow loads (< 0.12 N). In this method, the indenter is instrumented to provide independent determinations of force applied to the fiber and displacement of the fiber in the matrix. The revised method permits examination of both debonding and frictional sliding in a SiC/glass-ceramic composite. Values of τ_f on the order of 3.5 MPa were obtained on this material, in good agreement with the initial measurements using the Vickers diamond. One particular aspect of this method which limits its use is the special apparatus required to apply very small loads, although efforts are currently being made to expand the load range which can be applied [19]. While most of the work on the indentation push-in test has been conducted using a standard Vickers diamond geometry, Mandell et al [2] have shown that the shape of the indenting diamond can be changed to increase the amount of sliding which can be observed.

While the typical indentation push-in test uses the Vickers diamond to push the fiber into the matrix, the indentation push-out test uses the diamond to push the fiber through the matrix. The push-out test requires the use of thinner specimens ($< 2-3$ mm) than the push-in test. The basic assumptions in the analysis of the push-out test are the same as for the push-in test and also neglects stress concentrations at the bottom surface where the fiber emerges during the test. In the push-out test, three regimes are envisioned: an initial region in which the diamond is in contact with the fiber only and the sliding length is less than the thickness of the sample, a plateau region in which the sliding length is greater than or equal to the thickness of the sample, and a final region in which the diamond makes contact with and deforms

the matrix. These regimes are shown schematically in Figure 1. In principle, the initial regime also represents the behavior of the push-in test; however, the assumption that specimen thickness is much greater than the fiber diameter is not valid if the thickness is too small. In addition, the surface stress concentrations will play a larger role than in thicker samples. In the initial regime, τ is determined from the slope (m) of a plot of the force on the fiber squared (F^2) versus displacement (δ):

$$\tau = m/4\pi^2 R^3 E_f \quad (1)$$

where R is the radius of the fiber and E_f is the elastic modulus of the fiber. In the plateau region of the curve, τ is determined from the force at which the plateau occurs:

$$\tau = F/2\pi Rt \quad (2)$$

where t is the thickness of the specimen. In the last regime, where the diamond is in contact with the matrix, τ cannot be determined. Which value of τ (debond or frictional) is measured in the plateau region depends on whether or not there is a chemical bond between the fiber and matrix and what geometry indenter is being used. In the typical geometry using a standard Vickers diamond, when the fiber debonds, the frictional stress is also exceeded and the fiber slips until either contact with the surrounding matrix occurs or until friction slows the fiber displacement to a value expected from frictional stresses alone. If no debonding must occur, then only slippage due to friction is present.

For large monofilaments such as the SCS-6 SiC, where the SiC is deposited on a carbon core, two plateaus are expected. The first occurs when the carbon core (33 μm diameter) slips in the SiC; the second when the SiC fiber (about 140 μm diameter) slips in the matrix. The fiber displacements at which each of these events takes place can be calculated from the geometry of the

Vickers diamond. The diamond should make contact with the SiC at a displacement of about 5 μm , and it should contact the matrix at a displacement of 20 μm . Thus a plateau occurring prior to 5 μm can be attributed to the slippage of the carbon core, and one occurring prior to 20 μm can be attributed to slippage of the SiC. Whether one plateau or two plateaus occur depends on the debond strength of the interfaces between the core and SiC, and between the SiC and the surrounding matrix.

EXPERIMENTAL PROCEDURE

Single fiber pull-out samples were fabricated by sandwiching SiC monofilaments between borosilicate glass plates and heating under dead weight loading corresponding to 14-21 KPa pressure. Molybdenum sheets were placed between the dead weight and the glass plates to prevent adhesion during fabrication. The entire assembly was immersed in graphite powder to prevent oxidation of the fibers. Industrial grade argon was kept flowing through the furnace. The samples were held at 760°C for 60 min to obtain good flow of the glass around the monofilament. A schematic of the finished samples is shown in Figure 2. Different embedded lengths were obtained by varying the length of the monofilament between the plates. Individual samples were loaded in uniaxial tension on a screw-driven universal test machine⁴. The samples were gripped using swivel hooks attached to ball joints to facilitate alignment of the fiber with the stress axis. Samples were pulled at a rate of 0.05 cm/min. The embedded length was determined from the force-displacement curves (Figure 3), since accurate optical measurements prior to testing could not be made due to uncertainty in where the monofilament emerged from between the glass plates.

⁴ Instron Corp., Canton, MA.

The materials for the indentation tests were either obtained from commercial sources (glass-ceramic, see footnote 2) or made by hot pressing a sample of SiC/borosilicate glass at 800°C for 30 minutes at about 14 KPa. The indentation tests were performed using an instrumented indenter, allowing for independent determinations of force and displacement. A schematic of the test apparatus is shown in Figure 4. Displacement was determined using a pair of capacitance probes; the change in capacitance in a probe varies as it approaches a fixed target. Targets were fixed with respect to the specimen surface, and each probe was initially calibrated using a laser interferometer. Specimens for indentation included 1 mm and 2 mm thick multifilament SiC/glass-ceramic and 0.3 mm thick monofilament SiC/borosilicate glass. The samples were at least partially flat and polished so that the capacitance probes did not have to be adjusted frequently. A 50 g load was used for the SiC/glass-ceramic material, and the loads ranged from 130 to 150 g for the SiC/borosilicate material. Based on the debond strength of the SiC/glass, as determined from the single fiber pull-out test (9 MPa), loads < 140 g should exhibit a single plateau of the core slipping in the SiC while loads > 140 g should exhibit both plateaus.

RESULTS AND DISCUSSION

As noted above, which value of τ is measured depends on the test method employed as well as the material being tested. It is expected that the single fiber pull-out test will provide information on both debonding strength and frictional stresses, while the push-in test will measure frictional stresses only. The push-out test could measure either or both debond strength or frictional stress, depending on the material and the indenter geometry.

Two types of force-displacement curve were observed in the SiC monofilament/borosilicate glass system as shown in Figure 5. In both cases, the load increased linearly with displacement until the fiber debonded from the matrix. In the first case, there was a sharp drop in load, followed by pull-out of the fiber. In the second case, the load decreased gradually from the maximum while the fiber pulled out. The two types of curves may indicate two types of interface failure. A sudden drop indicates catastrophic failure of the entire interface whereas the smoother curve indicates a more gradual, incremental failure of the interface.

The maximum force required to initiate pull-out of the fiber vs embedded length is plotted in Figure 6. Although there is considerable scatter in the data, it can be seen that the pull-out force increases with increasing embedded length as long as the fiber strength is not exceeded. Some of the scatter may be due to non-uniform flow of glass around the fiber during hot pressing, leading to an air gap at the interface, and therefore reduced contact area and pull-out force. Also plotted in Figure 6 are the loads at which only frictional forces are acting on the interface. The difference between the maximum load and the frictional load is not constant. To confirm that the first load drop is due to debonding, several samples were unloaded following the initial load drop, then reloaded. Upon reloading, pull-out was observed at the same load where unloading had occurred, showing that the fiber-matrix bonds were in fact broken initially and that only frictional stresses were operating at the interface. Occasionally, after reloading, a very small load drop was observed which is attributable to the difference between the static and dynamic coefficients of friction. The stability of τ during pull-out over a wide range of instantaneous embedded length is demonstrated in Figure 7.

The values of τ_f measured using the single fiber pull-out test for the SiC/borosilicate system are lower than those obtained by Goettler and Faber [6] (12.5 MPa), but, as noted in the Background Section, the analytical methods were different, as were the specimen fabrication procedures. When the data of Deshmukh and Coyle [4] for SiC reinforced borosilicate glass are examined using the analysis of Equation 4, a value of τ_f of 22 MPa is obtained. When the expected residual stresses are taken into account (Equations 5a and 5b), a value of τ_0 between 7 and 18 MPa is found, depending on the choice of friction coefficient (0.2 vs 0.72). A friction coefficient of 0.72 is the value taken from reference 4, while $\mu = 0.2$ is that determined in reference 6. Both values of τ_0 are in good agreement with the result of Goettler and Faber for the same nominal composition matrix.

For the SiC/borosilicate glass system, the push-out test shows either one or two plateaus (Figure 8). As described above, based on the debond strength of SiC/glass, loads < 140 g should exhibit a single plateau while those > 140 g should exhibit two plateaus. The first case is shown in Figure 8a. The force at the plateau gives a value of τ_d of 38 MPa for the core slipping through the SiC. The second case is shown in Figure 8b, where the force at the first plateau gives a value of τ of 36 MPa for the core slipping in SiC and the force at the second plateau gives a value of τ of 10 MPa for the SiC slipping in the matrix. Tests on additional fibers gave an average value of τ of 30 ± 9 MPa for the core in SiC. The value of τ for SiC in the matrix is in reasonable agreement with τ_d obtained from the single fiber pull-out test. These results are based on a fairly small number of fibers and additional verification is required to more firmly establish these values. In addition to more data, precise measurements of the indentations need to be made and Marshall's analysis applied to the data to confirm that the two methods agree.

Examination of the SiC/glass-ceramic system shows that τ is dependent on the investigator as well as the technique. The indentation push-in results yield τ 's varying from 1 to 10 MPa, depending on the investigator [1,3-5,10] and from 1 to 100 MPa, depending on the heat treatment [4]. The discrepancy in heat treated materials is due to differences in the fiber-matrix interface bonding with some fibers being more tightly bound than others. This would lead to differences in both debond strength and frictional pull-out. The discrepancy in various untreated materials is due to both differences in the fiber-matrix bond and fiber misorientation with respect to the applied force.

In a sample which is 2 mm in thickness, the indentation test was either of the push-in or push-out type. Typical results are shown in Figure 9. In Figure 9a, a push-in type is shown while Figure 9b shows a push-out result. In both cases, however, τ is on the order of 1-6 MPa for this system, leading to the conclusion that this τ is due to frictional effects. Values of τ as high as 55 MPa were also observed, leading to the supposition that there are differences in the bonding between fiber and matrix at different locations in the specimen. The indentation push-out test results are more difficult to obtain because of the need to use flat and polished samples. Based on a number of measurements, however, the indentation push-out results are more reproducible than are the indentation push-in results. For this thickness sample, it is apparent that the assumptions for both types of test are met. For thinner samples, the assumption that the thickness \gg fiber diameter may be violated, thus τ_f determined from the plateau region of the push-out test may not agree with that obtained in the initial region where push-in is assumed to take place. The analysis of the push-out test in the plateau region is simpler than that required for the push-in test and is not affected

by the assumptions regarding elastic interactions after the force is released and what happens below the slip region during testing.

CONCLUSIONS

Each of the test methods discussed in this paper has advantages and disadvantages. The single fiber pull-out test provides the most direct method of determining the interfacial strengths, both debonding and frictional, but at present can only be used effectively for large fiber diameters, primarily due to specimen handling considerations. The indentation tests use a minimal amount of material and can be performed on samples containing either large monofilaments or small diameter multifilament tows but provide information on only τ_f (push-in) or τ_f or τ_d (push-out), depending on indenter geometry and material characteristics. It is possible that the push-out test can be performed at slower loading rates and with a different indenter geometry, thus allowing for separation of the debonding strength from the interfacial friction stress in the force²-displacement curve. The preparation of indentation push-out samples is more difficult than for indentation push-in samples but the analysis is simpler and the results appear to be more reproducible. While there are some discrepancies yet to be resolved, interfacial strengths determined using different test methods agree well with one another as do debond strengths determined using different methods. Based on the ability to measure both debond strength and interfacial frictional stress, and the need to use a minimal amount of material, the indentation push-out test appears to be the most desirable one to use.

ACKNOWLEDGEMENTS

The authors would like to thank S. W. Freiman, E. R. Fuller, Jr., M. J.

Koczak, and M. Barsoum for many helpful discussions. We are grateful to Dr. S. G. Fishman for support through SDIO/IST contract N00014-86-F-0096.

REFERENCES

- 1) Marshall, D. B., Journal of the American Ceramic Society, Volume 66, December, 1984, pp. C259-C260.
- 2) Mandell, J. F., Grande, D. H., Tsiang, T.-H., and McGarry, F. J., in Composite Materials: Testing and Design, ASTM STP 893, J. M. Whitney, ed., ASTM, Philadelphia, 1986, pp. 87-108.
- 3) Marshall, D. B., and Oliver, W. C., Journal of the American Ceramic Society, Volume 70, August, 1987, pp. 542-548.
- 4) Coyle, T. W., Chan, H. M., and Deshmukh, U. V., in Interfaces in Polymer, Ceramic, and Metal Matrix Composites, H. Ishida, ed., Elsevier, Amsterdam, 1988, pp. 489-501.
- 5) Deshmukh, U. V., Kanei, A., Freiman, S. W., and Cranmer, D. C., in High Temperature/High Performance Composites, MRS Symposium Volume 120, Materials Research Society, 1988.
- 6) Goettler, R. W., and Faber, K. T., Ceramic Engineering and Science Proceedings, Volume 9, 1988, pp. 861-870.
- 7) Harris, B., Morley, J., and Philips, D. C., Journal of Material Science, Volume 10, 1975, pp. 2050-2061.
- 8) Piggott, M. R., Sanadi, A., Chua, P. S., and Andison, D. in Composite Interfaces, H. Ishida and J. L. Koenig, Eds., Elsevier, Amsterdam, 1986, pp. 109-121.
- 9) Penn, L. S., and Lee, S. M., Fibre Science and Technology, Volume 17, 1982, pp. 91-97.

- 10) Deshmukh, U. V., and Coyle, T. W., Ceramic Engineering and Science Proceedings, Volume 9, 1988, pp. 627-634.
- 11) Griffin, C. W., Limaye, S. Y., Richerson, D. W., and Shetty, D. K., Ceramic Engineering and Science Proceedings, Volume 9, 1988, pp. 671-678.
- 12) Cox, H. L., British Journal of Applied Physics, Volume 3, March 1952, pp. 72-79.
- 13) Greszczuk, L. B., in Interfaces in Composites, ASTM STP 452, 1969, pp. 43-58.
- 14) Lawrence, P., Journal of Materials Science, Volume 7, 1972, pp. 1-6.
- 15) Gray, R. J., Journal of Materials Science, Volume 19, 1984, pp. 861-870.
- 16) Takaku, A., and Arridge, R. G. C., Journal of Physics D: Applied Physics, Volume 6, 1973, pp. 2038-2047.
- 17) Vedula, M., Pangborn, R. N., and Queeney, R. A., Composites, Volume 19, January, 1988, pp. 55-60.
- 18) Oel, H. J., and Frechette, V. D., Journal of the American Ceramic Society, Volume 69, April, 1986, pp. 342-346.
- 19) Lowden, R. A., Oak Ridge National Laboratory, private communication, 1988.

Table 1

Frictional Shear Stress for Two Composite Systems

τ_f in MPa

(Numbers in parenthesis represent number of samples averaged)

<u>Technique</u>	<u>Reference</u>	<u>Nicalon/LAS III</u>	<u>SCS-6/Borosilicate</u>
Single Fiber Pull-Out			
Poisson's Contraction	5	-	3.6 ± 0.7 (9)
Residual Stress	6	-	15 - 28
Residual Stress-Free	6	-	12.5
Simple Analysis	10	-	5 - 6.5
Simple Analysis	This study	-	5.6 ± 2.7 (8)
Indentation Push-In			
Vickers Diamond	1	2.5 ± 0.9 (10)	-
Nanoindenter	3	3.5	-
Rapid Loading	3	2.1 ± 1.5 (70)	-
Vickers Diamond	4	1 - 100	-
Instrumented Indenter	This study	1 - 55	-
Indentation Push-Out			
Instrumented Indenter	This study	2 - 34	9 - 10

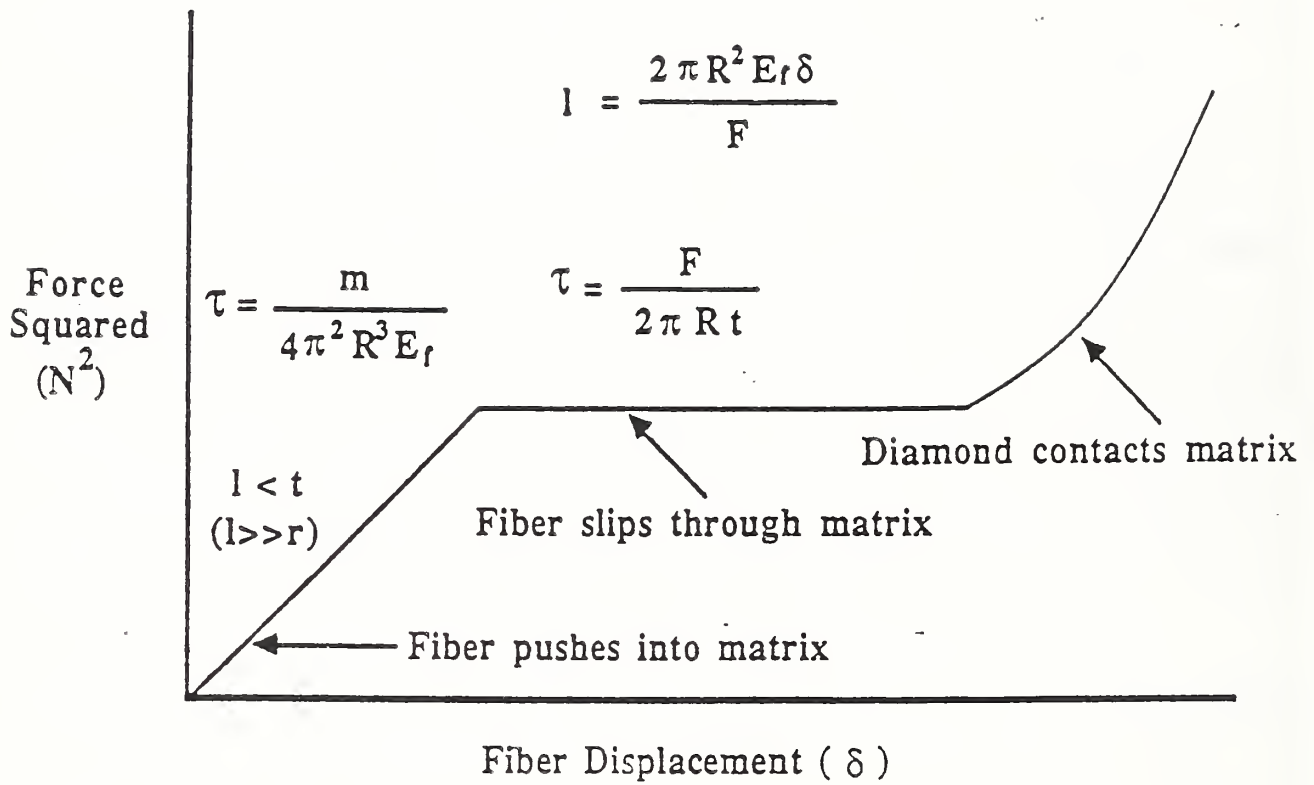


Figure 1. Schematic of force squared/displacement for indentation push-out test

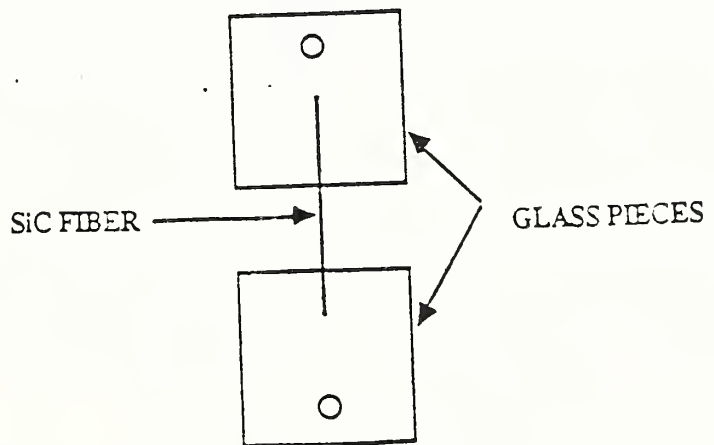
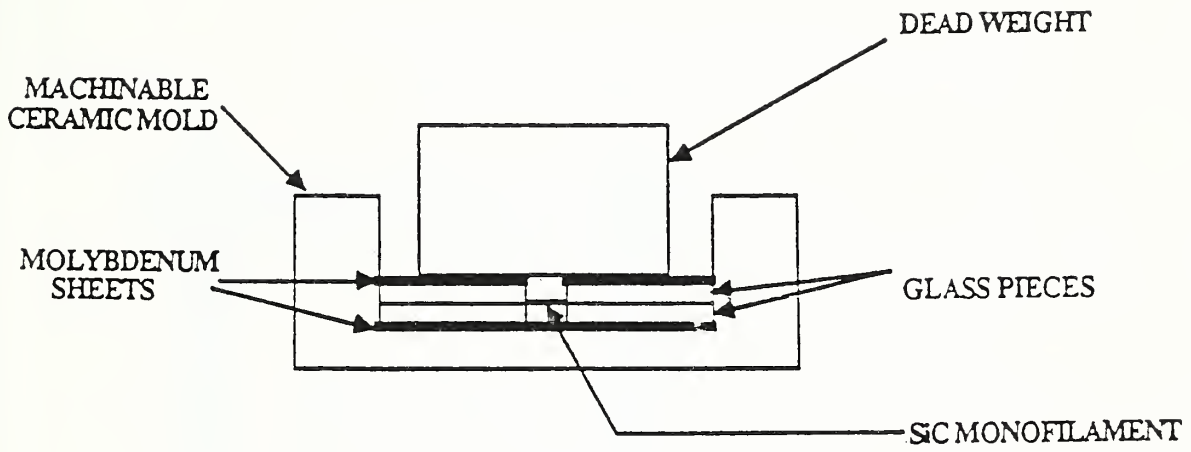


Figure 2. Schematic of the sample-making mold assembly and individual sample.

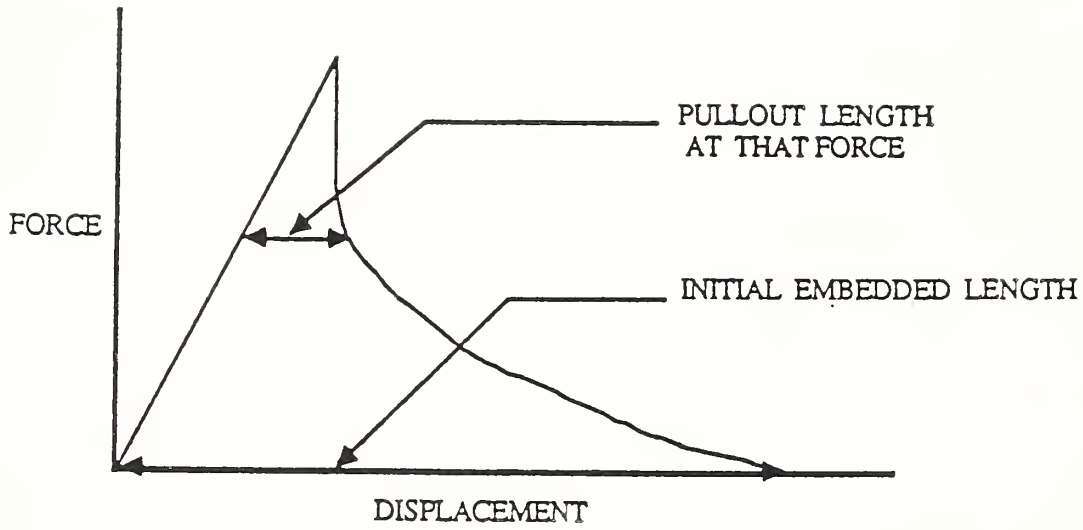


Figure 3. Measurement of pull-out and initial embedded length from a force-displacement curve.

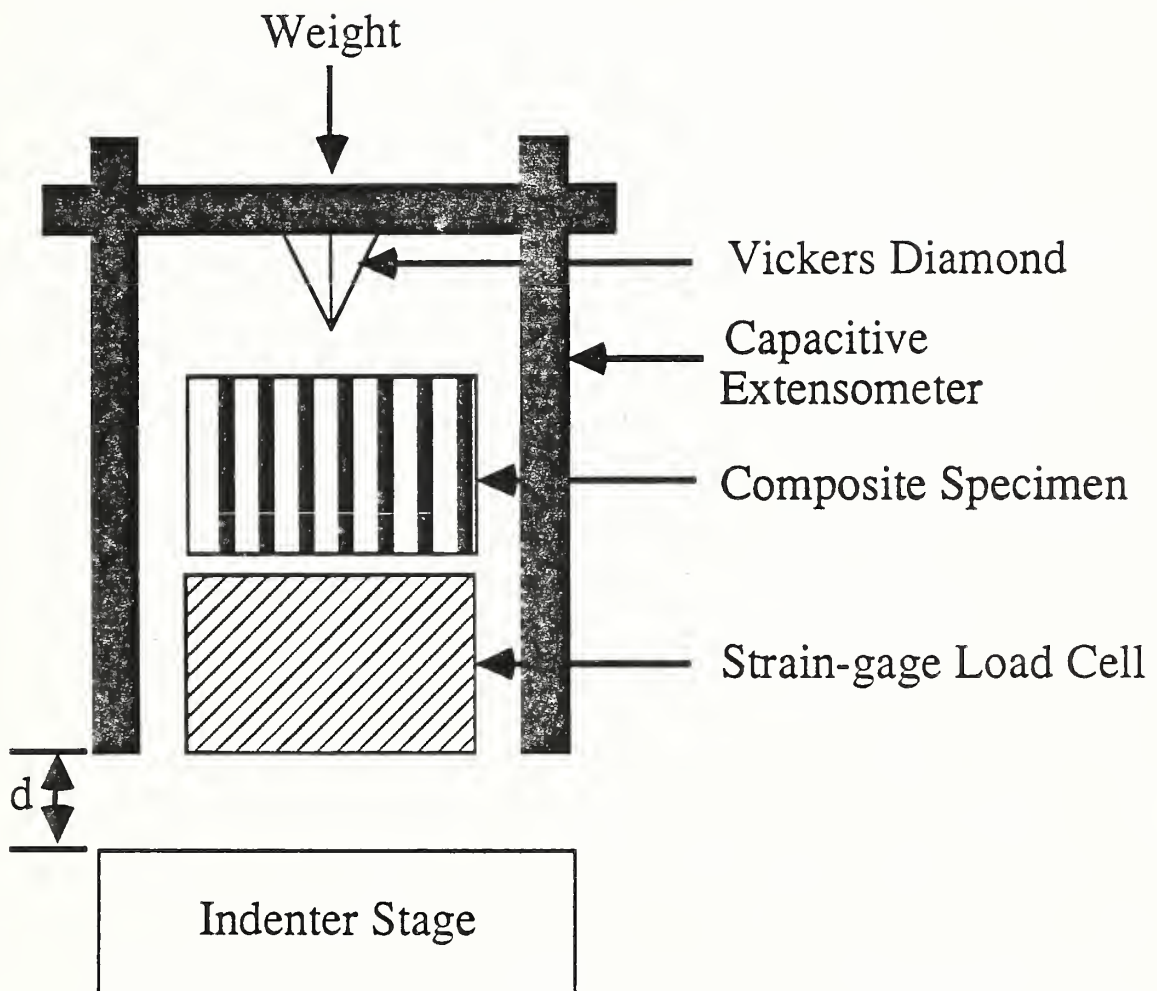


Figure 4. Schematic of indentation apparatus.

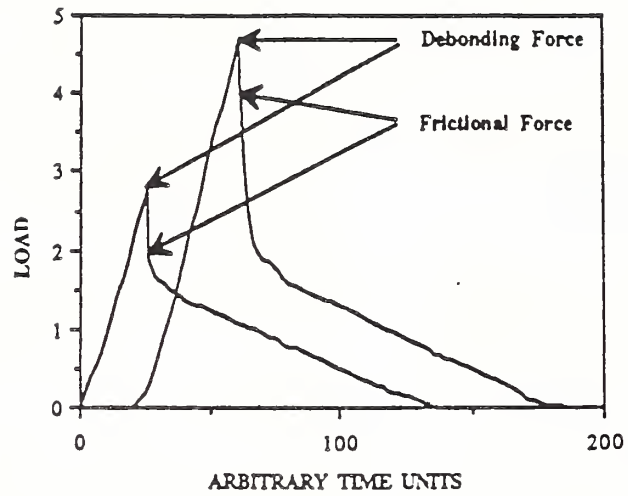


Figure 5. Typical force-time curves observed in SiC monofilament/borosilicate system.

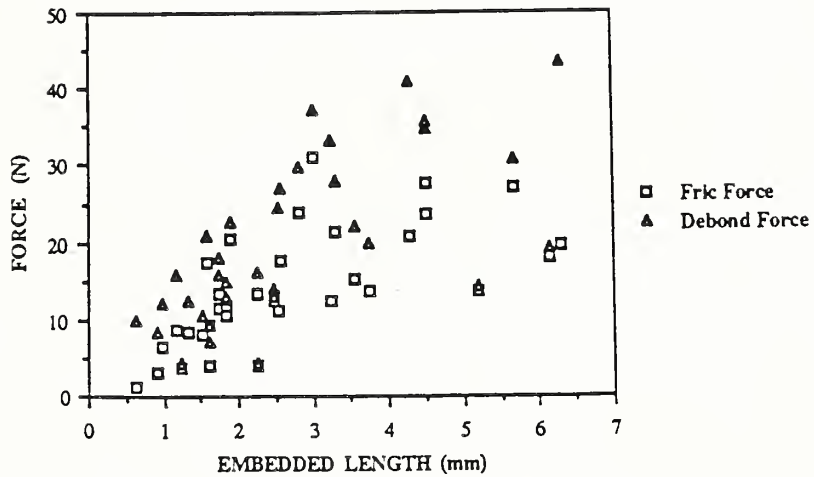


Figure 6. Plot of maximum pull-out force vs embedded length for SiC monofilament/borosilicate glass. Debond force is based on the maximum load observed during the test; frictional force is based on a lower load for which only frictional forces are operating on the interface.

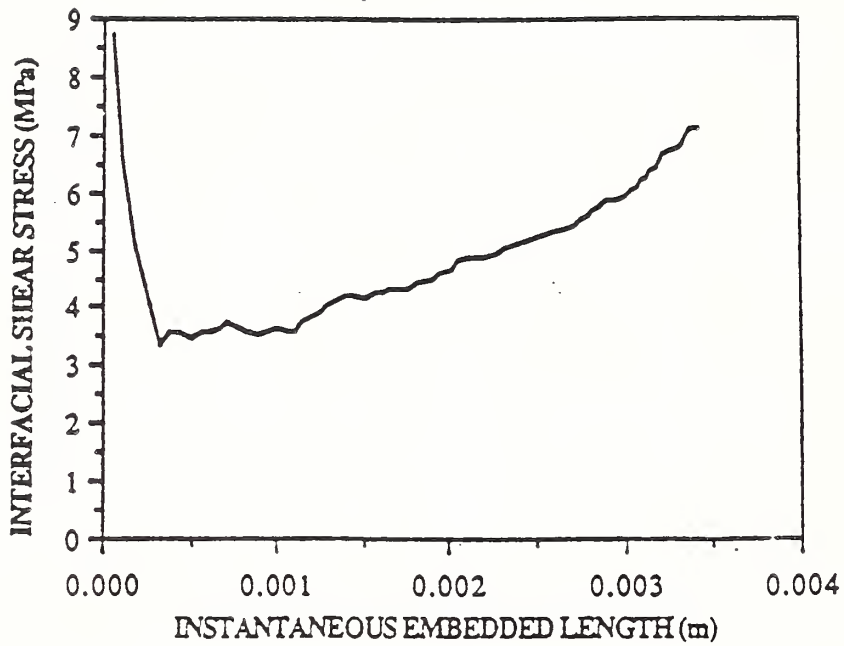


Figure 7. Plot of frictional stress throughout a single pull-out test as a function of instantaneous embedded length.

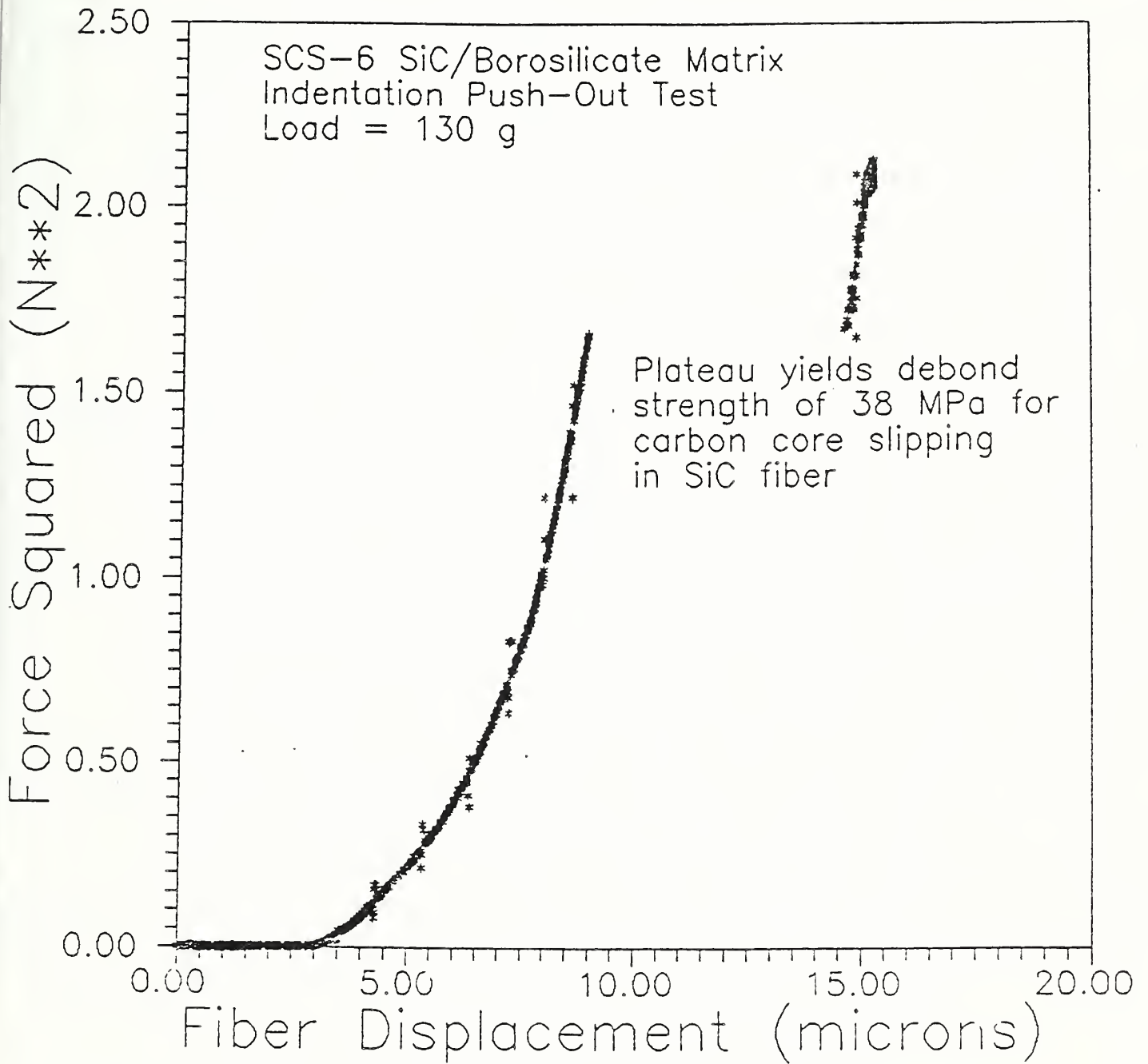


Figure 8. Results of indentation of SiC monofilament in borosilicate glass matrix.
 a. Indentation load = 130 grams.

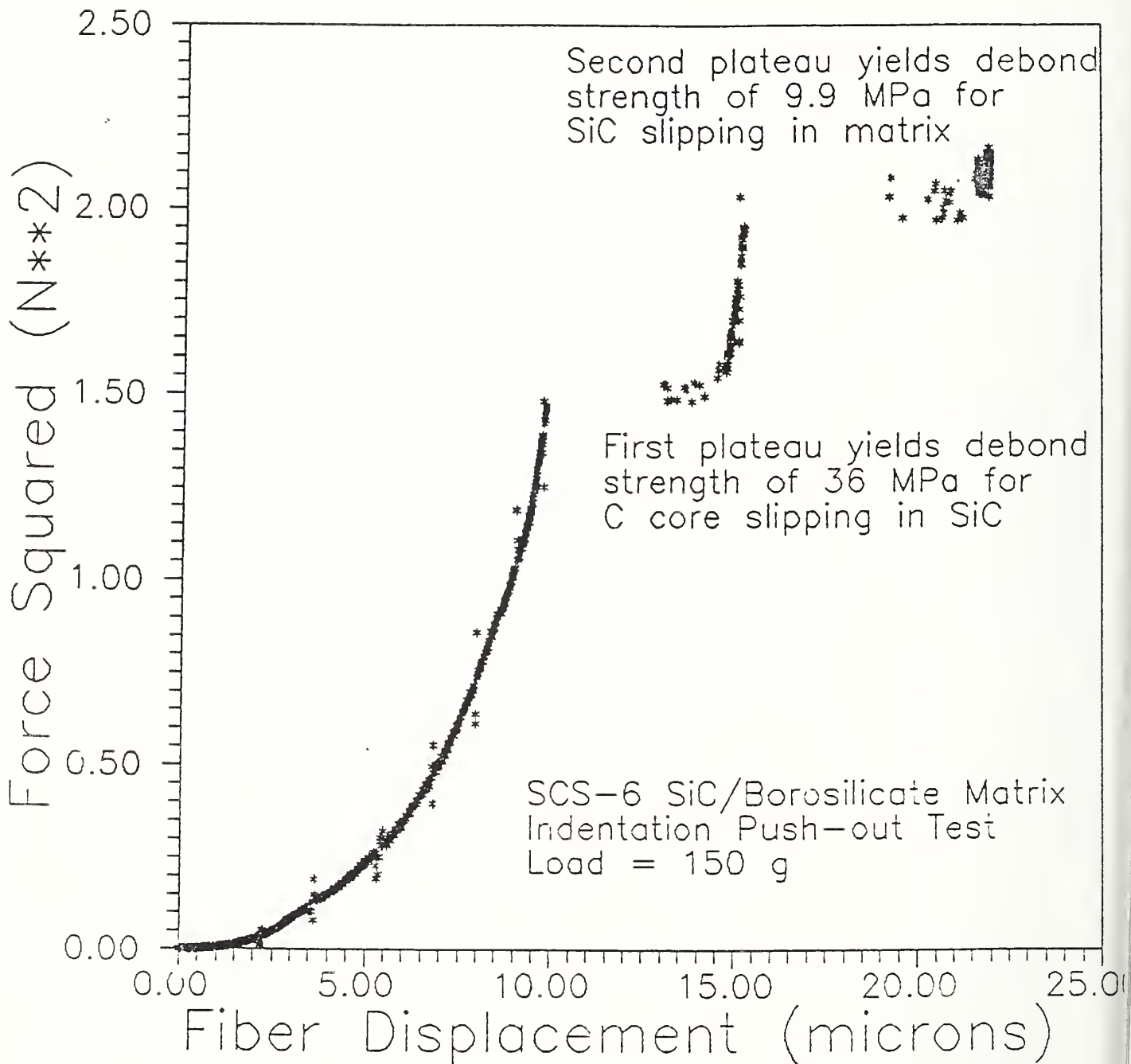


Figure 8. Results of indentation of SiC monofilament in borosilicate glass matrix.

b. Indentation load = 150 grams.

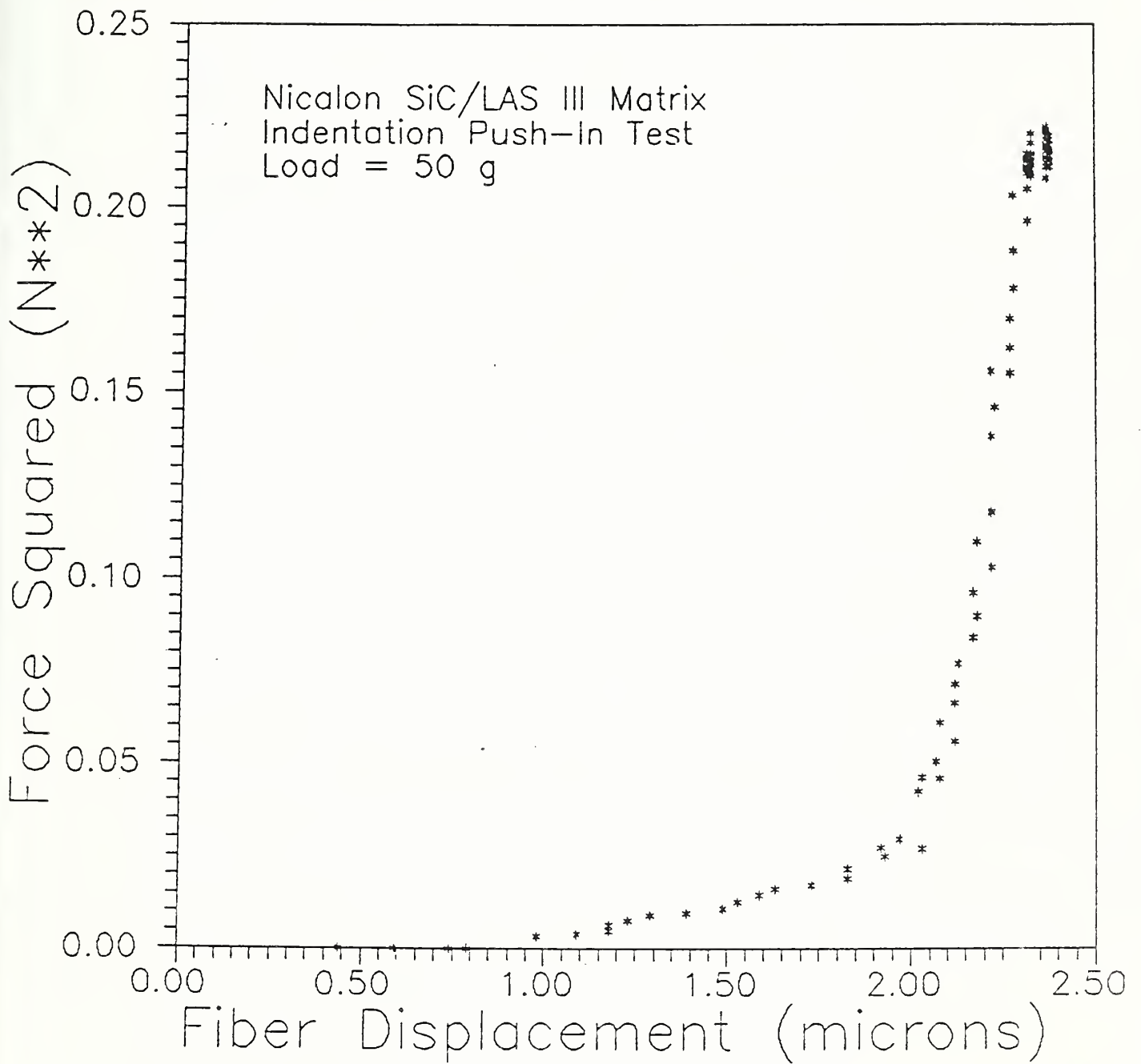


Figure 9. Results of indentation of SiC in lithium aluminosilicate matrix.

a. Push-in result ($l < t$)

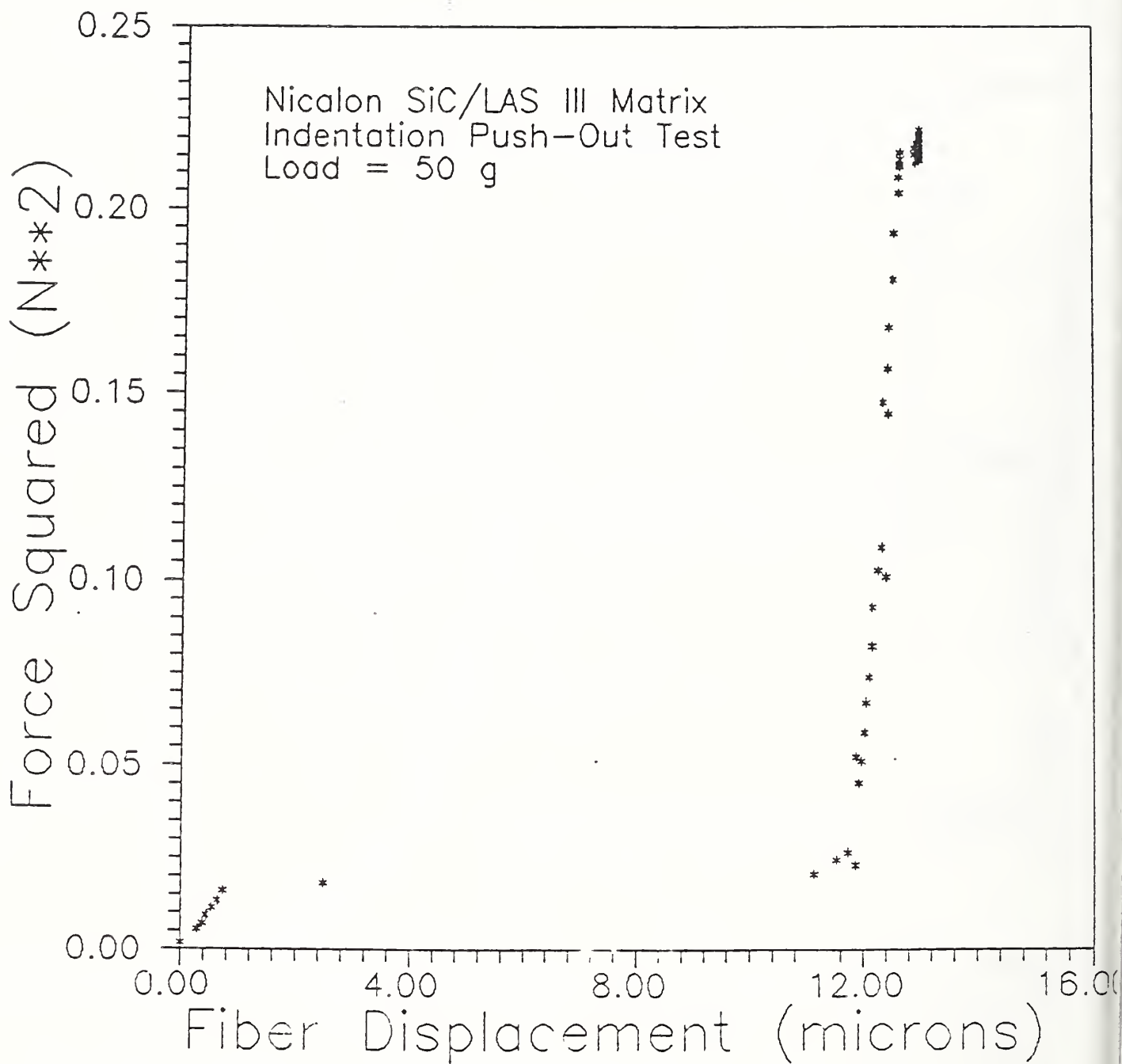


Figure 9. Results of indentation of SiC in lithium aluminosilicate matrix.

b. Push-out result ($l > t$)

A Perspective on Fiber Coating Technology

DAVID C. CRANMER

Ceramics Division
National Bureau of Standards
Gaithersburg, MD 20899

A variety of techniques exist for depositing coatings on ceramic and carbon fibers. This paper reviews several of these techniques and their advantages and disadvantages and points out several deficiencies in uniformly and reproducibly coating the fibers.

Introduction

In examining the key issues involved in developing high quality, tough ceramic matrix composites, one of the most important involves the chemistry and properties of the fiber-matrix interface. Determining appropriate interface composition and properties requires knowledge of the thermodynamics and kinetics of the overall composite (fiber-interface-matrix) system.^{1,2} Once an appropriate composition has been determined, appropriate toughening mechanisms can be explored.³⁻⁵ Both carbon and BN surfaces on SiC fibers have been shown to provide toughening behavior in some cases,¹⁻⁵ but it is unlikely that either is appropriate for extended use (> 10 hrs) at elevated temperatures (> 1000 °C) in an oxidizing environment.

The fiber-matrix interfacial region can be modified in several ways,³⁻⁶ but because of their versatility, only coating techniques will be considered for interface control. Many techniques exist for putting coatings on ceramic, carbon, and metal substrates. These methods have been reviewed in detail,⁷ but when fibers are the substrate, most of the more common methods cannot be used. The basic problem is that many coating methods rely on a line-of-sight between the source material and the substrate, which is not possible for uniformly coating fibers and fiber tows. Given the difficulties inherent in line-of-sight techniques, they will not be discussed further.

The most commonly used techniques for coating fibers are chemical vapor deposition (CVD), metal-organic precursor deposition, and polymer precursor deposition.^{8,9} Additional techniques such as electroless plating¹⁰ and electrodeposition¹¹ can also be used. Each technique has distinct advantages and disadvantages, which will be discussed below.

Chemical Vapor Deposition

CVD is a vapor transport technique wherein a chemical reaction occurs and the product is deposited on a substrate. There are three types of deposition, two limited by gas diffusion (either of reactants in or products out) and one limited by the reaction rate of the gases to form the deposit. The dominant process is determined by the partial pressure of the reactants and gaseous products, the chemical reactions, and the temperature of the reactor. For coatings, it is preferable to be gas-diffusion limited rather than reaction-rate limited. If the gases react to form the product before reaching the surface as occurs in the reaction-rate limited regime,

the particles produced may not adhere to the fiber or may clump on the surface.

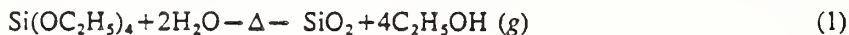
CVD is the most common method currently used for producing coatings on fibers. It uses a fairly simple apparatus (Fig. 1) but requires cleaning of the exhaust gases. A large number of compositions can be deposited with this technique.¹² The coating thickness can range from nanometers to several micrometers, depending on the length of the furnace and/or the number of CVD cycles to which the fibers are exposed. A distinct advantage of the technology is that the fiber coatings can be deposited on a continuous basis, allowing it to be combined with other composite fabrication techniques such as filament winding.

The uniformity of the coating is determined by the ability of the reactant gases to reach the fiber surfaces and the temperature at which the reaction is gas-diffusion limited. The CVD process is a slow one, but methods such as multiple cyclings of the fiber through the deposition chamber can be envisioned which may speed the overall coating process.

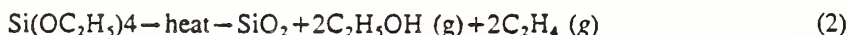
Metal-Organic Precursor

The metal-organic precursor (or sol-gel) process typically uses an alkoxide or mixture of alkoxides dissolved in a solvent which coats the fibers and then is made to undergo a chemical reaction to form the final product. The basic technique (Fig. 2) involves drawing the fiber or tow through a bath of the appropriate alkoxide(s), followed by hydrolysis or ammonialysis of the solution to convert the alkoxide to the oxide or nitride, followed by higher temperature treatments to pyrolyze/vaporize any remaining organic materials. Most of the coatings which have been produced to date are simple oxides.

Experience with this technique has shown that single layers of about 150 nm can be produced repeatedly.¹³⁻¹⁵ The compositional limits imposed on this process come from the available starting chemicals and the reactions to form the products. The chemistry of these systems can be straightforward as in the case of SiO₂ where



and



In more complicated multicomponent systems, different constituents may react or precipitate at different times, leading to inhomogeneities in composition or nonuniform thickness.

For thicker coatings (>200 nm), multiple dippings of the fibers are required.¹⁴ While this is a disadvantage for coatings of the same composition, it is very easy to obtain a graded composition coating using this technique. Like the CVD process, this technique can be used to continuously apply the coating to the fibers.

Polymer Precursors

In concept, this technique is almost identical to the metal-organic precursor technique described above. The difference is that a polymer or oligoimer in an appropriate solvent is used (not an alkoxide), and the coated fiber is pyrolyzed to form the ceramic. The apparatus is virtually identical to that shown in Fig. 2 except that the hydrolyzing furnace is removed from the system. The coating composition depends on the specific polymer precursor. This technique has been used to make carbon coatings from pitch precursors¹⁵ and SiC coatings from polycarbosilane.⁹ Other coatings which can be made by this technique will depend on the

availability of polymer precursors.^{15 16} This method also lends itself to being a continuous process.

Electroless Plating and Electrodeposition

Electroless plating¹⁰ and electrodeposition¹¹ provide methods for applying metallic coatings. They require a conductive fiber surface for deposition to take place, which can be achieved for some fibers but not for most of those available. They are relatively slow processes and require some clever engineering to make into continuous processes due to the need of a surface charge. Done properly, they provide a uniform coating of metal but their utility for coating multifilament tows is unclear since the effects of interacting surface charges are not known at this point.

Summary

The descriptions and discussions given above show that each of the coating techniques can be used to provide useful materials within certain limits. Almost any desired composition can be applied to a useful thickness using one or more of the techniques. What is still required to design coating systems is a better definition of the coating's purpose (diffusion barrier, reaction inhibitor, or something else), knowledge of the thermodynamics/kinetics of the overall system, as well as methods of coating characterization.

References

- ¹P. M. Benson, K. E. Spear, and C. G. Pantano, "Interfacial Characterization of Glass Matrix/Nicalon SiC Fiber Composites: A Thermodynamic Approach," presented at the 12th Annual Conference on Composites and Advanced Ceramic Materials, Cocoa Beach, FL 17-20 Jan. 1988.
- ²K. E. Spear, P. M. Benson, and C. G. Pantano, "Thermochemical Modeling for Interface Reactions in Carbon-Fiber Reinforced Glass Matrix Composites," to be published in the Proceedings of the 172nd Meeting of the Electrochemical Society.
- ³J. J. Brennan, "Additional Studies of SiC Fiber Reinforced Glass-Ceramic Matrix Composites," Technical Report, ONR Contract N00014-82-C-0096, 14 Feb., 1983.
- ⁴J. J. Brennan, "Interfacial Characterization of Glass and Glass-Ceramic Matrix/Nicalon SiC Fiber Composites," in *Tailoring Multiphase and Composite Ceramics*, R. E. Tressler, G. L. Messing, C. G. Pantano, and R. E. Newnham, eds., Plenum Press, New York, 1986, pp. 549-560.
- ⁵B. Bender, D. Shadwell, C. Bulik, L. Incorvati, and D. Lewis, "Effect of Fiber Coatings and Composite Processing on Properties of Zirconia-Based Matrix SiC Fiber Composites," *Am. Cer. Soc. Bull.*, 65 [2], 363-369 (1986).
- ⁶K. M. Prewo and J. J. Brennan, "High-Strength Silicon Carbide Fibre-Reinforced Glass-Matrix Composites," *J. Mat. Sci.*, 15 (1980) 463-468.
- ⁷T. E. Schmid, "High Technology Ceramic Coatings—Current Limitations—Future Needs," presented at the 12th Annual Conference on Composites and Advanced Ceramic Materials, Cocoa Beach, FL, 17-20 Jan. 1988.
- ⁸R. N. Singh and M. K. Brun, "Effect of Boron Nitride Coating on Fiber-Matrix Interactions," *Cer. Sci. Eng. Proc.*, 8 [7-8], 636-643 (1987).
- ⁹H. Katzman, "Fiber Wetting and Coatings for Composite Fabrication," SD-TR-86-63, The Aerospace Corporation, Oct. 1986.
- ¹⁰L. S. Evans and P. E. Morgan, "Method for Producing a Metal Composite," U. S. Patent 3 550 247, 29 Dec. 1970.
- ¹¹D. S. Lashmore, "Electrodeposition,"
- ¹²*Chemical Vapor Deposition, Second International Conference*, J. M. Blocher, Jr., and J. C. Withers, eds., The Electrochemical Society, New York, 1970, 861 pp.
- ¹³D. C. Cranmer and D. J. Speece, "Fiber-Matrix Interactions in Carbon Fiber/Cement Matrix Composites," in *Tailoring Multiphase and Composite Ceramics*, R. E. Tressler, G. L. Messing, C. G. Pantano, and R. E. Newnham, eds., Plenum Press, New York, 1986, pp. 609-614.
- ¹⁴H. Katzman, "Pyrolyzed Pitch Coatings for Carbon Fiber," U. S. Patent 4 376 804, Mar. 1983.
- ¹⁵F. Hurwitz, L. Hyatt, J. Gorecki, and L. D'Amore, "Silsequioxianes as Precursors to Ceramic Composites," *Cer. Sci. Eng. Proc.*, 8 [7-8], 732-743 (1987).
- ¹⁶K. J. Wynne and R. W. Rice, "Ceramics via Polymer Pyrolysis," in *Annual Reviews of Materials Science* 1984, Vol. 14, 1984, pp. 297-334.

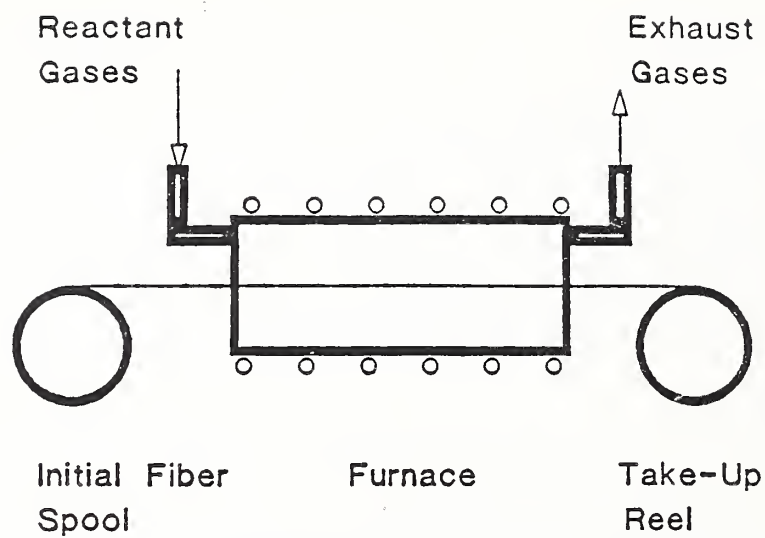


Fig. 1. Schematic of chemical vapor deposition apparatus for fiber coating.

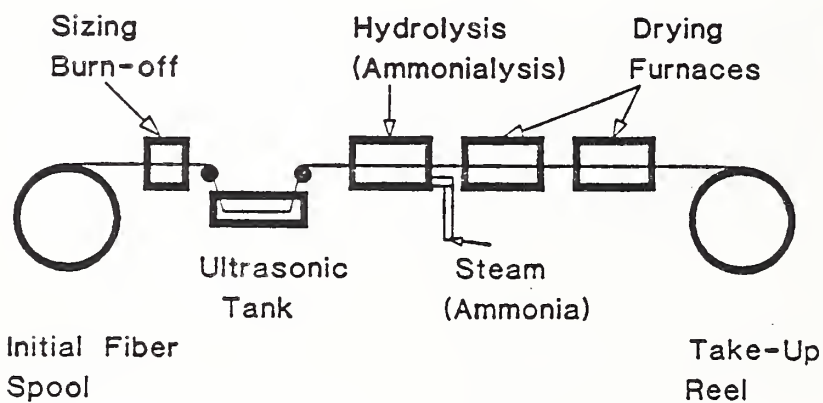


Fig. 2. Schematic of metal-organic precursor apparatus for fiber coating.

Fiber Coating and Characterization

DAVID C. CRANMER*

Ceramics Division, National Institute of Standards and Technology, Gaithersburg, MD 20899

In examining the key issues involved in developing high-quality, damage-tolerant ceramic-matrix composites, one of the most important areas involves the chemistry and properties of the fiber-matrix interface. Determining appropriate interface compositions and properties requires knowledge of the thermodynamics and kinetics of the overall composite (fiber-interface-matrix) system. In particular, the reactions that will occur to give the desired interface and the competing reactions that will impede or prevent the acquisition of the desired interface must be known, as well as how fast each of the reactions occurs. The thermodynamics describes in large part whether the necessary interface can be obtained whereas the kinetics provides an indication of the required processing time and temperature. In addition, the thermodynamics and kinetics provide some insight as to what service environment (temperature and atmosphere) and duration of exposure the composite will survive. Examples of the use of the thermodynamics and kinetics as aids to understanding composite fabrication and properties can be found in the literature.¹⁻³

When an appropriate composition has been determined, it then remains to determine whether the interfacial properties, especially the bond strength (mechanical or chemical), are suitable to provide an appropriate toughening mechanism (e.g., fiber pullout). As has been noted many times before,⁴⁻⁶ an interfacial bond that is too weak will result in a weak material whereas a bond that is too strong results in composites that will fail catastrophically. Both carbon and boron nitride surfaces on SiC fibers have been shown to meet the thermodynamic/kinetic criteria and provide the required toughening behavior^{1,2,4-6} at room temperature and at somewhat elevated temperatures. However, either coating is probably not appropriate for extended use (>10 h) at elevated temperatures (>1000°C) in an oxidizing environment. The same can be said of most other nitride- and carbide-coating compositions.

Controlling Interfacial Chemistry

The fiber-matrix interfacial region can be modified in several ways including in situ modification of the fiber surface to

yield a carbon-rich surface,⁴ additions to the matrix that segregate to the fiber surface,^{4,5} and coating of the fiber.^{6,7} From the standpoint of ease of fabrication, in situ modification to form the appropriate interface would be ideal. Unfortunately, such modifications are typically nonuniform, can lead to an undesired interfacial material, and can dramatically lower the strength of the fibers.⁸⁻¹¹ Additionally, the composition of the fiber itself may have to be modified to provide the desired interface material. Given the current state-of-the-art in making such fibers, it is not clear that such modifications can successfully be incorporated into the fabrication process. (For examples of the difficulties that can be encountered in fiber fabrication, consult Refs. 8 to 12.) The use of additives that will segregate to the interface has been successfully demonstrated,⁵ but relies on mass-transport processes (e.g., diffusion) that may be slow, or competing reactions may prevent the additive from segregating uniformly at the fiber surface.

The easiest, most versatile method for controlling the chemistry of the interface appears to be via the application of coatings to the fiber or tow prior to lay-up and fabrication of the composite. Assuming that the issue of *what* coating to apply has been resolved, a number of techniques exist for putting a variety of coating compositions on ceramic, carbon, and metal substrates.

These methods and their advantages and disadvantages have been reviewed in detail;¹² however, when fibers are the substrate, most of the more common methods cannot be used, especially when considering multifilament tows. The basic problem is that many coating methods rely on a line-of-sight between the source material and the substrate on which the material is being deposited. For monofilaments, this line-of-sight deposition is generally not available, unless multiple sources are used. For multifilament tows, even multiple sources do not solve the problem because the individual fibers will block one another from the source. Although spreading of the tows may help, the spreading-unspreading process may damage the fibers, thus reducing their ability to carry load in the composite.

Coating Techniques

The most commonly used techniques for coating fibers^{14,15} are chemical vapor deposition (CVD), sol-gel or organometallic precursor deposition, and polymer

precursor deposition. Additional techniques such as electrodeposition and electroless plating¹⁶⁻¹⁸ or line-of-sight techniques such as ion implantation or physical vapor deposition can also be used. Each of these techniques has distinct advantages and disadvantages, which will be discussed below. Also to be discussed are the methods of characterizing the coatings in terms of thickness, chemical composition, and properties.

Chemical Vapor Deposition

CVD is a technique that uses vapor transport of gaseous components that react and deposit the product(s) on a substrate. There are generally three regimes of behavior: two are limited by gas diffusion (either of reactants in or of products out), and one is limited by the reaction rate of the gases to form the deposit. The controlling regime is determined by the partial pressures and flow rates of the reactants and gaseous products, the chemical reactions, and the temperature of the CVD reactor. For coatings, it is preferable to be in either of the gas-diffusion-limited regimes, not in the reaction-rate-limited regime, for the following reason: if the gases react to form the product before reaching the surface (reaction-rate-limited regime), the particles produced may not adhere to the fiber or may provide a site at which clumps may form on the surface, resulting in a nonuniform layer.

CVD is probably the most common method currently used for producing coatings on fibers. It uses a fairly simple apparatus as shown in Fig. 1, but requires the use of scrubbers or other methods to clean the exhaust gases. A large number of compositions including carbides, nitrides, and oxides can be deposited with this method.¹⁹ The coatings can be made in thicknesses ranging from nanometers to several micrometers, depending on the length of the furnace and/or the number of CVD cycles to which the fibers are exposed.

A distinct advantage of the technology is that the fiber coatings can be deposited on a continuous basis, allowing them to be combined with other composite fabrication techniques, such as filament winding. Since the technique relies primarily on gaseous transport, coating all of the fibers in a tow is initially straightforward, provided that the deposition is made in the gas-diffusion-limited regime. However, as the coating process continues, the coating layers can grow to thick-

*Member, American Ceramic Society.

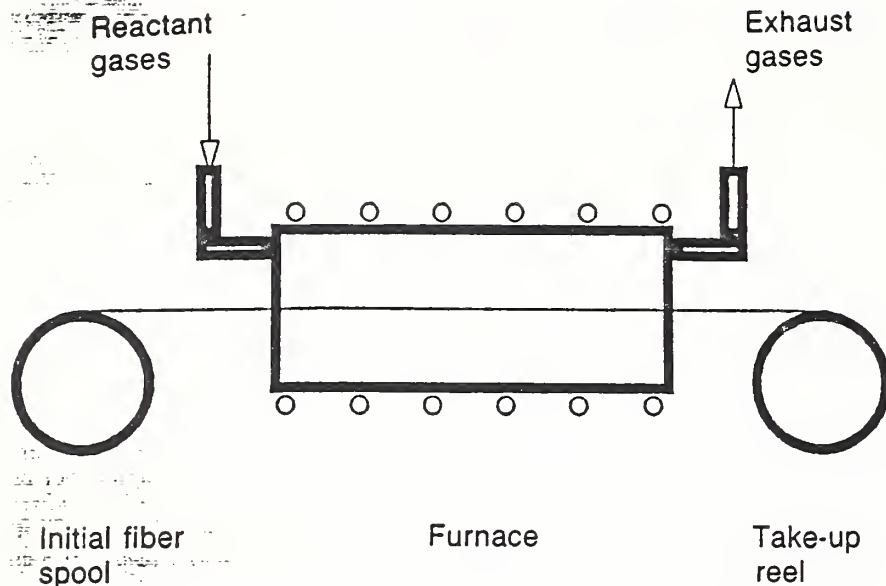


Fig. 1. Schematic of chemical vapor deposition apparatus for fiber coating.

nesses at which gas transport into the tow is constricted, resulting in nonuniformities in the final product. Taken to an extreme, this process results in a composite known as a chemically vapor infiltrated (CVI) composite.²⁰⁻²² Compositionally, limits are imposed on the process by the types of gases available and the complex reaction chemistries that occur in the reactor.

The uniformity of the coating is determined by the ability of the reactant gases to reach the fiber surface and the temperature at which the reaction is gas-diffusion limited. The process of getting the reactant gases to the fiber surfaces is controlled by reactant-gas partial pressure, total reactor pressure, reactor geometry, and fiber architecture. The latter is particularly important when dealing with a twisted fiber tow. Such a tow must be spread to expose individual fibers, but the spreading process may introduce flaws in the surface of the fiber, thus degrading the final composite due to fiber degradation rather than enhancing it due to the properties of the coating.

The temperature at which the coating is applied is critical. Temperature con-

trols both the thermodynamics and kinetics of the process. It must be maintained so that the reaction occurs on the fiber, not in the gas phase, and with an appropriate microstructure (grain size and shape). Small changes in the temperature ($\pm 25^\circ\text{C}$) may change the reaction and/or its kinetics, resulting in an inferior coating. An additional problem with the CVD process is the time required to make deposits. It is a slow process with deposition rates in the 1 to 10 $\mu\text{m}/\text{min}$ range, but methods such as multiple cyclings of the fiber through the deposition chamber can be envisioned, which may speed up the overall coating process.

Organometallic Precursor

The organometallic precursor (or sol-gel) process typically uses an alkoxide or mixture of alkoxides dissolved in a solvent. This liquid is used to coat the fibers, then undergoes a chemical reaction to form the final product. The basic technique is shown in Fig. 2 and involves drawing the fiber or fiber tow through a bath of the appropriate alkoxide(s), followed by hydrolysis of the solution to convert the alkoxide to the oxide, which is then followed

by higher temperature treatments to pyrolyze or vaporize any remaining organic materials. The basic process can be modified to produce nitrides by replacing the steam in the hydrolysis step with ammonia. However, most of the coatings that have been produced to date are oxides such as SiO_2 and Al_2O_3 .

Experience with this type of coating technique has shown that single layers of about 150 nm can be produced repeatedly.^{15,23,24} The compositional limits imposed on this process come from the available starting chemicals and the reactions to form the products. As with the CVD process, ventilation to remove toxic exhaust gases such as organic solvents is required. For thicker coatings (> 200 nm), multiple dippings of the fibers are required.²⁴ It is also easy to obtain a graded composition coating using this technique. A distinct disadvantage to multiple dippings, however, is the potential for cracking between layers, due to either inadequate processing or thermal expansion mismatch stresses. Like the CVD process, this technique can be used to continuously apply the coating to the fibers.

Polymer Precursors

In concept, the polymer precursor technique is almost identical to the organometallic precursor technique described above. The difference is that instead of using alkoxide or similar materials, a polymer or oligomer in an appropriate solvent is used, and instead of exposing the coated fiber to water or ammonia, it is pyrolyzed to form the ceramic. The apparatus is virtually identical to that shown in Fig. 2, except that the hydrolyzing furnace is removed from the system. The coating composition depends on the polymer precursor chosen. This technique has been used to make carbon coatings from pitch precursors²⁵ and SiC coatings from polycarbosilane.¹⁵

Other coatings that can be made by this technique will depend on the availability of polymer precursors. At present, these appear to be limited to systems that will result in Si-O-C-N, Si_3N_4 and, perhaps, Si-Al-O-N materials.²⁶⁻²⁸ Like the CVD and organometallic precursor techniques, this method is also a continuous process. An extension of this technique would be to use inorganic glasses as the precursors, which would be deposited at elevated temperatures. The exact compositions that would be useful have not been identified at this time, but one example is the family of glasses used for joining Si_3N_4 and SiC.²⁹

Electrodeposition and Electroless Plating

The electrodeposition and electroless plating techniques provide methods¹⁶⁻¹⁸ for applying metals if it is decided that a metallic coating is needed. Electrodeposition or electroplating is a process of metal deposition from a solution (including fused

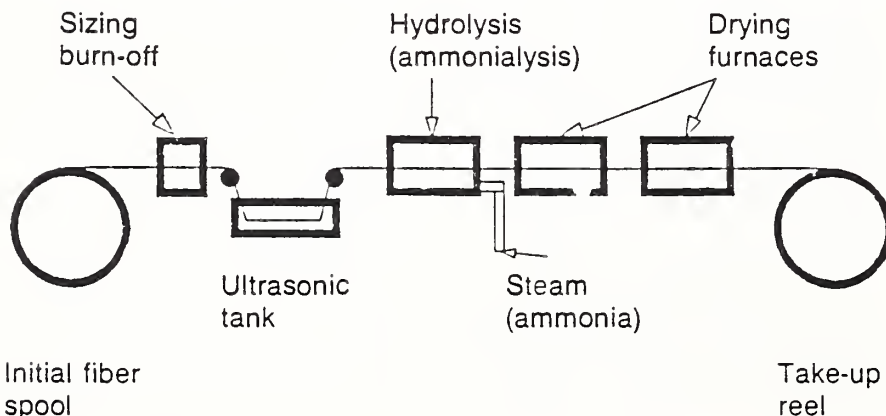


Fig. 2. Schematic of organometallic precursor apparatus for fiber coating.

salts) via electrolysis. The process requires the presence of both an anode to supply electrons to reduce the metallic ion(s) in solution to metal and a cathode on which to deposit the metal. In the present case, the fiber or tow acts as the cathode. Although a conductive fiber might be preferred, methods are available for striking an initial conductive coating onto a nonconductive substrate, which should permit its use with any fiber type. This technique has been used at the National Institute of Standards and Technology (formerly National Bureau of Standards)³⁰ to produce Ni coatings on SiC monofilaments for a mechanical test program. It is also being used commercially to produce copper-coated graphite fibers.³¹

Electroless plating uses no electrodes, but rather relies on a chemical reducing agent in solution to supply the electrons required to produce the metallic deposit. It is a relatively slow process, which requires that the deposition surface be autocatalytic (capable of initiating and sustaining the desired reaction). If this is done properly, it will provide a uniform coating of metal, but its use for coating multifilament tows is unclear, since the effects of interacting surfaces are not known at this point.

Line-of-Sight Techniques

A number of techniques are included in this category such as sputtering, physical vapor deposition, ion implantation, and electron-beam evaporation. The common thread in all of them is that they require a direct path from the source to the substrate. Although they are all relatively simple techniques to set up and use, they would not be useful for multifilament tows in which direct access is either not possible or very difficult to achieve due to the blocking effects of the fibers on one another.

For single filaments such as the AVCO monofilaments or spread tows, it may be possible to use multiple targets, or the fibers could be rotated somehow to expose them to the depositing material. The need for such a rotation or multiple targets could lead to difficulties in uniformity of the coating and its chemical homogeneity. In addition, these techniques do not appear to be appropriate for the type of continuous processing that would be desirable for a large-scale composite program, although it is conceivable that it could be done.

Coating Characterization

To achieve a composite that has both adequate strength and damage tolerance, the thickness and composition of any coating must be controlled. The reasons

for this are related to the need for a bond strength between fiber and matrix that allows load transfer from the matrix to the fiber below a minimum threshold strain and permits fibers to pull out of the matrix during fracture, thus contributing to graceful failure of the material. To ensure uniformity of the coating both in terms of thickness and chemical composition, some method of characterization must be used, preferably during or immediately after the coating has been applied. Unfortunately, at present there do not appear to be any techniques that are used for coating characterization on a continuous process basis.

The most common techniques for examining coatings on fibers, either after they are deposited or after they are incorporated into the matrix are electron microscopy (i.e., scanning electron microscopy (SEM) and transmission electron microscopy (TEM)) and scanning Auger microscopy (SAM).^{4,5,23,32} Unfortunately, these techniques are limited to examining very small areas at any one time, making it impossible to use these techniques for other than research pur-

poses. The information gained from these techniques is substantial, however, and can be used at some future date to correlate with other continuous scanning processes that may be developed.

Examples of the types of information that can be gained from SEM and SAM are shown in Figs. 3 to 5. Figure 3 shows a micrograph of a carbon fiber that has been coated with SiO₂ using the organometallic precursor process. The thickness of the coating can be determined from fracture surfaces as can its uniformity (smoothness) as shown in the figure.

Figures 4 (a survey scan of a carbon-coated Nextel 400* fiber surface) and 5 (a depth profile of the same coated fiber) show typical SAM results. The survey scan indicates that the carbon layer is present, but is thin enough to allow the Auger electrons of the fiber to be emitted and measured. It is obtained by scanning the specimen over a period of time and analyzing the Auger electrons emitted during the scan. The Al, Si, O, and B are all contained in the fiber, whereas C is due to the coating, making it impossible to use these techniques for other than research pur-

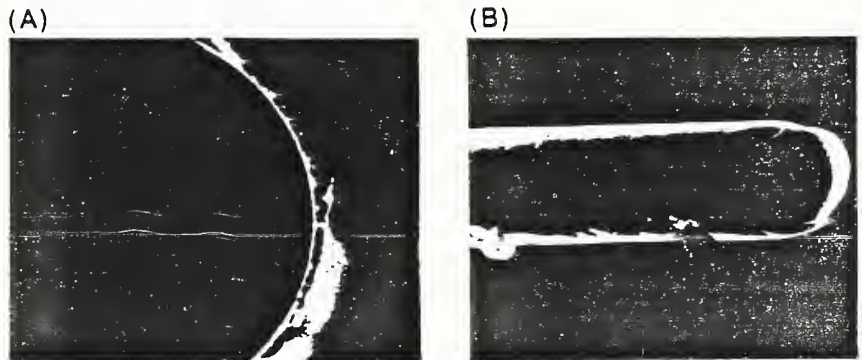


Fig. 3. SEM of carbon fiber coated with SiO₂. Coating thickness can be measured from the fracture surface, coating uniformity from the side view. (Photograph, courtesy of The Aerospace Corporation, El Segundo, CA) (A = 3000x; B = 1000x)

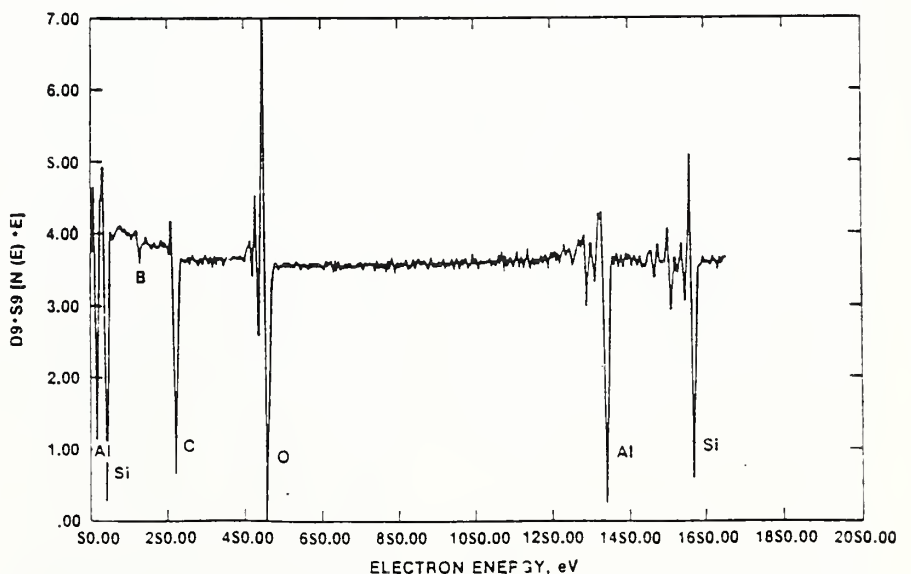


Fig. 4. Scanning Auger survey spectrum of carbon-coated Nextel 440 showing the presence of Al, B, C, O, and Si. Al, B, O, and Si are present in the fiber; C is the coating material.

*Nextel, 3M Company, St. Paul, MN.

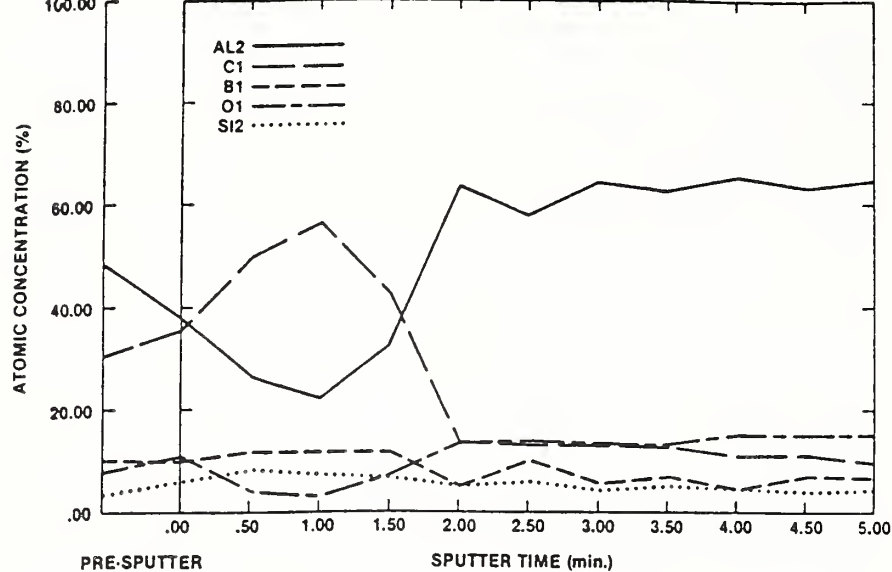


Fig. 5. Scanning Auger depth profile of carbon-coated Nextel 440 showing atomic concentration versus sputter time. Sputter time can be converted to coating thickness if sputter rate is known. Coating thickness in this case is about 30 nm.

ions for a known time to remove material. When the sputtering rate is known or measured, the time axis can be converted to depth.

The profile in Fig. 5 shows how thick the carbon layer is in any particular location. Repeated profiling at various locations would reveal the uniformity in thickness of the coating as well as the presence of any impurities in either the fiber or the coating. The implications of these results for the particular composite involved (mullite-mullite) are explained in more detail elsewhere.³³

Following fabrication or service, the same techniques can be used to determine how the fiber-matrix interface chemistry and thickness have changed. When these techniques are coupled with the mechanical properties techniques to be described later, they provide a reasonably complete picture of the composite behavior.

Several potential methods for determining thickness and composition in real time can be envisioned. One possible method for determining thickness involves continuously scanning the coated fiber with a laser of an appropriate wavelength (probably ultraviolet), with a detector mounted opposite the laser. The detector would be used to measure the thickness via either scattering or diffraction patterns generated as the light passes through the coating. Such signals could then be correlated with thickness measurements made using techniques such as the scanning Auger. Other methods involving electrical conductivity or resistivity can also be envisioned, if a means for maintaining electrical contact can be established in the process.

A method for continuously monitoring composition might be laser Raman spectroscopy³⁴ or Fourier transform infrared spectroscopy (FTIR).^{24,35} Both methods would use infrared (IR) wavelengths to scan the coated fiber and the Raman-induced vibrations or IR vibrations used to identify the composition, as compared with signals generated from standard reference materials. The FTIR method has been shown to be sensitive to SiO₂ coatings generated on SiC fibers by thermal oxidation.

Characterization of the coating before it is incorporated into the composite is only half the story. Additional postfabrication characterization of the fiber-coating-matrix interface is also required to ensure that the coating has been properly transformed into the desired interface material with the desired properties. The key property of interest is the fiber-matrix interfacial strength. This property consists of two separate components, namely, a debonding strength (τ_d) at which any chemical bond between fiber and matrix is released, and an interface stress (τ_f) at which the fiber pulls smoothly out of the matrix.

τ_f also has two components dictated by a static and a dynamic coefficient of friction. Several experimental methods including indentation push-in,³⁶⁻⁴⁰ indentation push-out,⁴⁰ and single-fiber pullout⁴¹⁻⁴³ tests have been used to characterize both the debonding strength as well as the frictional stress. The indentation tests can be performed using an instrumented indenter, thus allowing for independent determinations of force and displacement.

The advantage of the instrumented indenter over the method of Marshall³⁶ is that the sizes of the indentations, which are very small and the measurement of which is a significant source of error, do

not have to be measured directly. Specific composite systems that have been examined include glass (Na₂O-B₂O₃-SiO₂, Na₂O-CaO-SiO₂) matrices reinforced by SiC monofilaments (SCS-6)[†] and a glass-ceramic (LAS-III) matrix reinforced by SiC fibers (Nicalon).[‡]

In general, there is reasonable agreement between the values of τ_f measured using the different methods. Single-fiber pullout test results gave τ_f of 2 to 12.5 MPa for the SiC/Na₂O-B₂O₃-SiO₂ system and 4 to 20 MPa for the SiC/Na₂O-CaO-SiO₂ system.⁴³ τ_f increased in going from the Na₂O-B₂O₃-SiO₂ to the Na₂O-CaO-SiO₂ system, due to the increase in thermal expansion difference ($\Delta\alpha = 6 \times 10^{-7}/^\circ\text{C}$ for SiC/Na₂O-B₂O₃-SiO₂ and $56 \times 10^{-7}/^\circ\text{C}$ for SiC/Na₂O-CaO-SiO₂), which in turn results in a higher clamping stress on the fiber, hence a larger τ_f . The differences in τ_f measured for the SiC/Na₂O-B₂O₃-SiO₂ system are currently ascribed to the different analytical methods used by different investigators.

The indentation push-in test gave values of τ between 2 and 34 MPa for the SCS-6-LAS-III system. The former value comes from the work of Marshall³⁶ whereas the latter is based on the work of Fuller et al.^{39,40} The range in τ is believed to be due to differences in bonding between the fibers and matrix at various locations in the samples. In the indentation pushout test, three regimes are known (Fig. 6): an initial region in which the diamond is in contact with the fiber only and the sliding length is less than the thickness of the sample, a plateau region in which the sliding length is equal to the thickness of the sample, and a final region in which the diamond makes contact with and deforms the matrix. The behavior of the fiber-matrix system in the initial region should be identical to that of the indentation push-in test. Values of τ between 1 and 55 MPa for the SiC-LAS-III composite were obtained using this push-out test.

The major limitation of all the indentation techniques, like those for chemical analysis, is that only small portions of the material can be examined at any given time. An additional constraint involves how well the diamond is centered on the fiber being indented. If the diamond is not centered, torques can be imposed on the fiber that will lead to artificially high values for both τ_d and τ_f . A third constraint is imposed by sample size and preparation. The samples are small (approximately 5 by 5 by 1 to 5 mm) and must be polished and reasonably parallel. Additional postfabrication chemical and structural characterization can be performed using the SEM/TEM and SAM techniques discussed earlier.

Extending the Limits

The descriptions and discussions given above show that each of the coating tech-

[†]Textron/AVCO, Lowell, MA.
[‡]United Technologies, East Hartford, CT

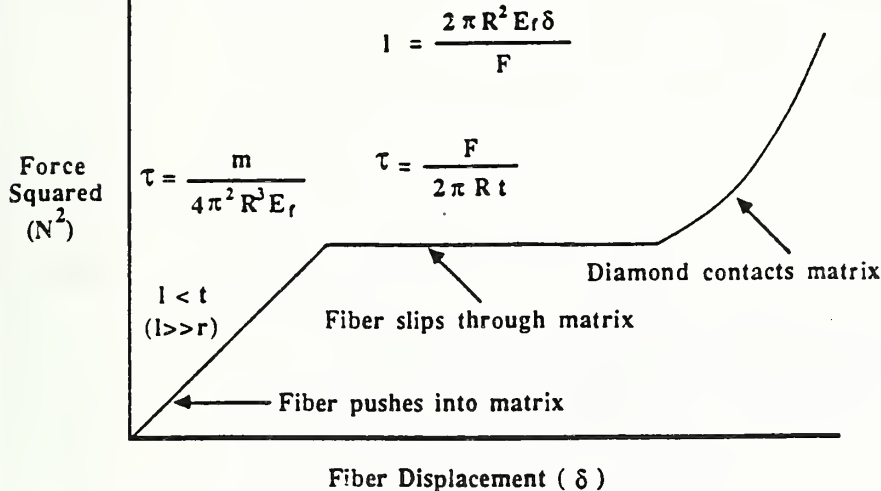


Fig. 6. Schematic of force squared versus displacement for the indentation push-out test showing the three regimes of behavior: diamond pushing on partially debonded fiber only (first regime); diamond pushing on fiber debonded along its entire length (second regime); diamond making contact with matrix (third regime).

niques can be used to provide useful materials within certain limits. By and large, almost any desired composition can be applied to a useful thickness, using one or more of the techniques. A better definition of the coating's purpose (e.g., is it a diffusion barrier, a reaction inhibitor, or something else?) and a good knowledge of the thermodynamics and kinetics of the fiber-coating-matrix system are still required. In particular, one of the components needed to successfully coat fibers uniformly is a method or methods of determining composition and thickness in real time.

Characterization methods are currently limited to those techniques that can examine small amounts of material and require time-consuming specimen preparation and/or expensive analysis equipment. Particularly in the mechanical properties area, understanding of the relationships between the simple test methods and real composite materials is limited. Real progress in this area will only be made when the correlation between the results of tensile tests (σ , ϵ) and push-in/push-out/pulbut tests (τ_p , τ_f) can be made and related to interfacial structure and chemistry.

References

¹P. M. Benson, K. E. Spear, and C. G. Pantano, "Thermochemical Characterization of Glass Matrix/Nicalon SiC Fiber Composites: A Thermodynamic Approach," *Ceram. Eng. Sci. Proc.*, 9 [7-8] 663-70 (1988).
²K. E. Spear, P. M. Benson, and C. G. Pantano, "Thermochemical Modeling for Interface Reactions in Carbon-Fiber-Reinforced Glass-Matrix Composites," pp. 345-54 in the Proceedings of the Electrochemical Society, Vol. 88-5, Electrochemical Society, New York, 1988.
³M. I. Mendelson, "SiC/Glass Composite Interphases," *Ceram. Eng. Sci. Proc.*, 6 [7-8] 612-21 (1985).
⁴J. J. Brennan, "Additional Studies of SiC-Fiber-Reinforced Glass-Ceramic Matrix Composites," Tech. Rept. No. R83-916018-2, Office of Naval Research Contract N00014-82-C-0096, 1983.
⁵J. J. Brennan, "Interfacial Characterization of Glass and Glass-Ceramic Matrix/Nicalon SiC Fiber Com-

posites"; pp. 549-60 in Tailoring Multiphase and Composite Ceramics. Edited by R. E. Tressler, G. L. Messing, C. G. Pantano, and R. E. Newnham. Plenum, New York, 1986.

⁶B. Bender, D. Shadwell, C. Bulik, L. Incorvati, and D. Lewis III, "Effect of Fiber Coatings and Composite Processing on Properties of Zirconia-Based Matrix SiC Fiber Composites," *Am. Ceram. Soc. Bull.*, 65 [2] 363-69 (1986).

⁷K. M. Prewo and J. J. Brennan, "High-Strength Silicon Carbide Fibre-Reinforced Glass-Matrix Composites," *J. Mater. Sci.*, 15, 463-68 (1980).

⁸T. J. Clark, M. Jaffe, J. Rabe, and N. R. Langley, "Thermal Stability Characterization of SiC Ceramic Fibers: I, Mechanical Property and Chemical Structure Effects," *Ceram. Eng. Sci. Proc.*, 7 [7-8] 901-13 (1986).

⁹L. C. Sawyer, R. T. Chen, F. Haimbach IV, P. J. Harget, and M. Jaffe, "Thermal Stability Characterization of SiC Ceramic Fibers: II, Fractography and Structure," *Ceram. Eng. Sci. Proc.*, 7 [7-8] 914-30 (1986).

¹⁰L. C. Sawyer, M. Jamieson, D. Brikowski, M. I. Haider, and R. T. Chen, "Strength, Structure, and Fracture Properties of Ceramic Fibers Produced from Polymeric Precursors," *J. Am. Ceram. Soc.*, 70 [11] 798-810 (1987).

¹¹R. W. Rice, J. R. Spann, D. Lewis, and W. S. Coblenz, "The Effect of Ceramic Fiber Coatings on the Room-Temperature Mechanical Behavior of Ceramic-Fiber Composites," *Ceram. Eng. Sci. Proc.*, 5 [7-8] 614-24 (1984).

¹²W. H. Atwell, W. E. Hauth, R. E. Jones, and N. R. Langley, "Advanced Ceramics Based on Polymer Processing," Tech. Rept. No. AFWAL-TR-84-4061, Air Force Wright Aeronautical Laboratories Contract F33615-83-C-5006, July, 1984.

¹³T. E. Schmid and R. J. Hecht, "High-Technology Ceramic Coatings—Current Limitations/Future Needs," *Ceram. Eng. Sci. Proc.*, 9 [9-10] 1089-94 (1988).

¹⁴R. N. Singh and M. K. Brun, "Effect of Boron Nitride Coating on Fiber-Matrix Interactions," *Ceram. Eng. Sci. Proc.*, 8 [7-8] 636-43 (1987).

¹⁵H. Katzman, "Fiber Wetting and Coatings for Composite Fabrication," Tech. Rept. No. SD-TR-86-63, AFSD Contract No. FO4701-85-C-0086-P00016, The Aerospace Corporation, 1986.

¹⁶F. A. Lowenheim, ed., *Modern Electroplating*, 3d ed. Wiley, New York, 1974, 801 pp.

¹⁷J. McDermott, *Electroless Plating and Coating of Metals*. Noyes Data Corp., Park Ridge, NJ, 1972, 303 pp.

¹⁸L. S. Evans and P. E. Morgan, "Method for Producing a Metal Composite," U.S. Pat. No. 3 550 247, Dec. 29, 1970.

¹⁹J. M. Blocher, Jr. and J. C. Withers, eds., *Chemical Vapor Deposition*, Second International Conference. The Electrochemical Society, New York, 1970, 861 pp.

²⁰D. P. Stinton, A. J. Caputo, R. A. Lowden, and T. A. Besmann, "Improved Fiber-Reinforced SiC Composites Fabricated by Chemical Vapor Infiltration," *Ceram. Eng. Sci. Proc.*, 7 [7-8] 983-89 (1986).

²¹D. P. Stinton, A. J. Caputo, and R. A. Lowden,

Chemical Vapor Infiltration, *Am. Ceram. Soc. Bull.*, 65 [2] 363-69 (1986).

²²P. J. Lamick, G. A. Bernhart, M. M. Dauchier, and J. G. Mace, "SiC/SiC Composite Ceramics," *Am. Ceram. Soc. Bull.*, 65 [2] 333-38 (1986).

²³D. C. Cranmer and D. J. Speece, "Fiber-Matrix Interactions in Carbon Fiber/Cement Matrix Composites"; pp. 609-14 in Tailoring Multiphase and Composite Ceramics. Edited by R. E. Tressler, G. L. Messing, C. G. Pantano, and R. E. Newnham. Plenum, New York, 1986.

²⁴J. J. Lannutti and D. E. Clark, "Sol-Gel-Derived Coatings on SiC and Silicate Fibers," *Ceram. Eng. Sci. Proc.*, 5 [7-8] 574-82 (1984).

²⁵H. Katzman, "Pyrolyzed Pitch Coatings for Carbon Fiber," U. S. Pat. No. 4 376 804, Mar., 1983.

²⁶F. I. Hurwitz, L. Hyatt, J. Gorecki, and L. D'Amore, "Silsesquioxanes as Precursors to Ceramic Composites," *Ceram. Eng. Sci. Proc.*, 8 [7-8] 732-43 (1987).

²⁷K. J. Wynne and R. W. Rice, "Ceramics via Polymer Pyrolysis"; pp. 297-334 in Annual Reviews of Materials Science 1984, Vol. 14, Annual Reviews, Inc., Palo Alto, CA, 1984.

²⁸B. G. Penn, F. E. Ledbetter III, and J. M. Clemmons, "An Improved Process for Preparing Tris (N-methylamino)methylsilane Monomer for Use in Producing Silicon Carbide-Silicon Nitride Fibers," *Ind. Eng. Chem. Process Des. Dev.*, 23 [2] 217-20 (1984).

²⁹D. B. Coon and R. M. Neilson, Jr., "Joining of Silicon Carbide-Reinforced Ceramics," Tech. Rept. No. ORNL/FMP-87/2, Apr. 1988, pp. 101-24.

³⁰S. W. Freiman, T. W. Coyle, E. R. Fuller, Jr., P. L. Swanson, D. C. Cranmer, and W. Haller, "Mechanical Property Enhancement in Ceramic Matrix Composites," Tech. Rept. No. NBSIR 88-3798, Apr. 1988.

³¹D. Lashmore, National Bureau of Standards, private communication, 1988.

³²R. Chaim and A. H. Heuer, "The Interface Between (Nicalon) Silicon Carbide Fibers and a Glass-Ceramic Matrix," *Adv. Ceram. Mater.*, 2 [2] 4-8 (1987).

³³O. Yeheskel, M. L. Balmer, and D. C. Cranmer, "Interfacial Chemistry of Mullite-Mullite Composites," *Ceram. Eng. Sci. Proc.*, 9 [7-8] 687-94 (1988).

³⁴The Instrumentation Sourcebook: A Compendium of Instruments and Techniques for Energy Research, DHR, Inc., prepared for U.S. Department of Energy Fossil Energy Office of Technical Coordination, Feb. 1986, pp. 112-13.

³⁵G. P. LaTorre, J. J. Lannutti, and D. E. Clark, "Hot-Stage Fourier Transform Infrared Reflection Spectroscopy of Sol-Gel-Derived Alumina," *Ceram. Eng. Sci. Proc.*, 5 [7-8] 506-12 (1984).

³⁶D. B. Marshall, "An Indentation Method for Measuring Matrix-Fiber Frictional Stresses in Ceramic Composites," *J. Am. Ceram. Soc.*, 67 [12] C-259-C-260 (1984).

³⁷D. B. Marshall and W. C. Oliver, "Measurement of Interfacial Mechanical Properties in Fiber-Reinforced Ceramic Composites," *J. Am. Ceram. Soc.*, 70 (8) 542-48 (1987).

³⁸K. T. Faber, S. H. Advani, J. K. Lee, and J.-T. Jinn, "Frictional Stress Evaluation along the Fiber-Matrix Interface in Ceramic Matrix Composites," *J. Am. Ceram. Soc.*, 69 [9] C-208-C-209 (1986).

³⁹E. R. Fuller, Jr., T. W. Coyle, R. F. Krause, Jr., and T. J. Chuang, "Structural Reliability and Damage Tolerance of Ceramic Composites for High-Temperature Applications," Tech. Rept. No. NBSIR 87-3564, Apr. 1987.

⁴⁰T. W. Coyle, T. R. Palamides, S. W. Freiman, E. R. Fuller, and U. V. Deshmukh, "Crack-Fiber Interactions in Ceramic Matrix Composites"; to be published in Proceedings of the American Society for Metals. American Society for Metals, Metals Park, OH.

⁴¹U. V. Deshmukh and T. W. Coyle, "Determination of the Interface Strength in Glass-SiC Composites via Single-Fiber Tensile Testing," *Ceram. Eng. Sci. Proc.*, 9 [7-8] 627-34 (1988).

⁴²R. W. Goettier and K. T. Faber, "Interfacial Shear Stresses in SiC- and Al₂O₃-Fiber-Reinforced Glasses," *Ceram. Eng. Sci. Proc.*, 9 [7-8] 861-70 (1988).

⁴³U. V. Deshmukh, A. Kanei, D. C. Cranmer, and S. W. Freiman, "Effect of Thermal Expansion Mismatch on Fiber Pull-out in Glass Matrix Composites," in High-Temperature/High-Performance Composites, MRS Symposium Volume 120, Edited by F. D. Lemke, A. G. Evans, S. G. Fishman, and J. R. Strife. MRS, Pittsburgh, PA, 1988.

Trade names and companies are identified in this paper in order to adequately specify the materials and equipment used. In no case does such identification imply that the products are necessarily the best available for the purpose.

Interfacial Chemistry of Mullite-Mullite Composites

ORI YEHESKEL,* MARI LOU BALMER, AND DAVID C. CRANMER

Ceramics Division
National Bureau of Standards
Gaithersburg, MA

Interfacial chemistry of mullite fiber reinforced-mullite matrix composites was examined using SEM/EDX and scanning AES. All the fibers bond strongly to the matrix and exhibit no sliding during a fiber push-in test. Excess Si over Al is found at the fiber-matrix interfaces. AES results show the carbon layer is nonuniform and in some cases less than 30 nm thick.

Introduction

The key to obtaining strength and toughness in ceramic matrix composites lies in the ability to control the chemistry and properties of the fiber-matrix interface. In these materials, the bond between the fiber and matrix should be such that the fibers are difficult to pull out of the matrix but not so strong that cracks propagate unimpeded across the fibers and matrix. Carbon and boron nitride coatings have been shown to provide the necessary interfacial properties.^{1,2}

Mullite ($3\text{Al}_2\text{O}_3 \cdot 2\text{SiO}_2$) has potential application as a radome material³ but one deficiency⁴ in the monolithic form is its low fracture toughness (K_{Ic}). Improvement of K_{Ic} from $2.2 \text{ MPa} \cdot \text{m}^{1/2}$ to $4.7 \text{ MPa} \cdot \text{m}^{1/2}$ was reported⁴ through the addition of 20 vol% SiC whiskers. Although a considerable improvement, the addition of 20 vol% SiC whiskers may adversely affect the dielectric properties. The present study was undertaken to examine the possibility of producing mullite matrix composites reinforced by continuous mullite fibers.

Experimental Procedures

Three different mullite fibers were used in this study: Nextel 480, Nextel 440, and carbon-coated (by a CVD process) Nextel 440.† Fiber phase composition was determined by X-ray diffraction. Additional characterization was done using SEM with EDX analysis. Carbon-coated Nextel 440 fiber was examined in a scanning Auger microprobe. The composites were fabricated by laying each set of fibers between previously cold-pressed (25 MPa) mullite powder bars,‡ which were then cold-pressed (50 MPa), wrapped with Mo foil, and hot pressed in a graphite die (Ar atmosphere of 0.1 MPa at $1465 \pm 10^\circ\text{C}$, 27 MPa, 1 hour). The three resulting composites were separated from one another with a diamond wafering blade. Density was determined by Archimedes' method in distilled water. Microhardness of the fibers and matrices was determined using the method of Marshall,⁵ which is an indentation push-in test, at loads of 0.5, 1, and 2 N. The composites were examined in the SEM after being coated with a thin layer of carbon to reduce charging and permit data acquisition for chemical microanalysis by EDX.

*On leave from NRCN, Israel.

†3M Corp., Ceramic Materials Dept., St. Paul, MN.

‡High Purity Mullite 193-CR, Baikowski International, Charlotte, NC.

Results and Discussion

Indentation

Examination of the fiber indentations showed that no movement had occurred. In many cases, cracks which initially developed in the dense fibers propagated from the indentation site into the less dense matrix, suggesting that the bond between the fiber and matrix is a strong chemical bond. Figure 1(A) shows an indent in the middle of a carbon-coated 440 fiber, where blunting of the cracks in the matrix can be seen. Figure 1(B) shows 1 N indent on one fiber in a 440 bundle, where the cracks extend into the matrix and on into the fiber bundle. Figure 1(C) shows various 1 N indents in a bundle of Nextel 480 fibers; crack extension is evident. Table I summarizes the hardness values of the fibers and matrices. The hardness of single fibers in the less dense matrix is always less than in the dense fiber bundle. The results show that the hardness increases with decreasing indentation load. Similar findings of increasing hardness with decreasing loads have been reported in ceramics.^{6,7} Differences in matrix hardness are probably due to density differences arising from the hot pressing process. The composite density ranges from 82 to 87%. Given the lack of fiber motion, additional chemical information on the fiber-matrix interface is discussed below.

Interface Chemistry

Figures 2(A-C) show the X-ray diffraction patterns of the three fibers. Analysis (Table II) shows that the 480 fibers consist of mullite and a minor amount of an amorphous phase. The 440 fibers contain mullite, an amorphous phase, and η - Al_2O_3 . The coated 440 contains less amorphous phase and more mullite than does the uncoated 440, suggesting that mullite was formed at the expense of the amorphous phase during coating.

EDX analysis showed that a stoichiometric mullite matrix was not present except in the Nextel 440 fiber-containing sample, all other cases showed an excess of Si over Al. Since the carbon layer may preferentially absorb the Al X-rays, a correction factor (CF) was incorporated into the compositional analyses. The CF was determined by calculating the ratio between the theoretical stoichiometric mullite (28.25 wt% SiO_2) and the calculated SiO_2 wt% content determined from the measured Si value in each matrix. The CF was multiplied by the calculated wt% SiO_2 in the fibers. Al_2O_3 content is assumed to be 100 wt% SiO_2 . The corrected values of SiO_2 and Al_2O_3 are shown in Table II.

Uncorrected EDX line scans and corresponding micrographs along a bare Nextel 480 fiber, across two Nextel 480 fibers in the composite, and across one Nextel 440 fiber in the composite are shown in Figs. 3(A-C), respectively. Figure 3(A) shows a homogeneous distribution of Al and Si along the fiber as well as a systematic variation in Si and Al, representative of an apparent layered structure in the fiber. The scans in Figs. 3(B) and 3(C) show that the interfaces between fiber and matrix and between fiber and fiber contain larger amounts of Si than Al. Si is probably present as a (boro)silicate, resulting in a strong chemical bond across the interfaces. However, the interface composition was not determined because the precise boron content could not be measured due to interference from the carbon coating.

Figure 4 shows the AES survey scan of the carbon-coated Nextel 440 fiber. In addition to C from the coating, the elements present in the fiber (Si, Al, B, and O) are all evident. The fact that the fiber elements are seen prior to sputtering indicates that the coating is thin (≤ 30 nm). Survey scans taken at other points do not show the fiber elements without surface removal, indicating a nonuniform

coating. Analysis of the energy peak location⁸ shows that Si is present in a covalent environment (Si or SiC) while Al is present in a metallic or carbidic form (Table III). Al is assumed to be present as the carbide. The peak shape of the carbon indicates that it is present as carbidic material, not as a hydrocarbon. Figure 5 shows the depth profile of the coated fiber. The sputtering rate of carbon is about 12.5 nm/min, thus the coating in this location is about 25 nm thick. On sputtering through the surface layer, the carbon concentration increases to a peak, while the Al and O contents decrease and the Si and B contents increase slightly. At depths greater than that corresponding to the carbon concentration peak, the carbon content decreases steadily to a constant value, the Al and O concentrations increase significantly to approximately constant values, and the Si and B contents decrease slightly. After most of the carbon layer has been removed, the variation of Al, Si, and B is systematic, indicative of a layered structure as was seen in Fig. 3(A). The depth profile indicates that carbon atoms diffused into the interior of the fiber.

Conclusions

The results of this study showed that the fibers did not move during the push-in test. Cracks extend unimpeded from the fibers to the matrix and from fiber to fiber within fiber bundles. This behavior is indicative of a strong interfacial bond between fiber and matrix and between fiber and fiber. The end result is that no toughening of the mullite material would be expected. The surface chemical composition of the fibers changes from a homogeneous distribution of Al and Si prior to hot pressing to an inhomogeneous, Si-rich material in the studied composites. These interfaces most likely consist of a borosilicate glass composition.

The carbon coating on the Nextel 440 fibers, which was expected to provide the necessary interface properties, was either too thin or too nonuniform to act as the appropriate interface. Auger results showed that the fiber's major constituents diffused through the carbon during the coating process, enabling or enhancing the formation of a strong chemical bond between the fibers and matrix.

Acknowledgments

We would like to thank Dr. Allan Holtz of 3M for supplying the carbon-coated Nextel 440 fibers, to Dr. Alexander Shaprio of NBS/Metallurgy Div. for assisting in the SEM/EDXA work, and to DARPA/DSO for funding this work.

References

- ¹B. Bender, D. Shadwell, C. Bulik, L. Incorvati, and D. Lewis III, *Amer. Cer. Soc. Bull.*, **65** [2] 363-369 (1986).
- ²K. M. Prewo and J. J. Brennan, *J. Mat. Sci.*, **15** (1980) 463-468.
- ³D. P. Partlow, W. R. Brose, and C. A. Andersson, AFWAL-TR-85-4152, April 1986.
- ⁴P. F. Becher, T. N. Tiegs, J. C. Ogle, and W. H. Warwick in *Fracture Mechanics of Ceramics, 7: Composites, Impact, Statistics, and High Temperature Phenomena*, R. C. Bradt, A. G. Evans, D. P. H. Hasselman, and F. F. Lange, eds., Plenum, New York, 1986, pp 61-73.
- ⁵D. B. Marshall, *J. Amer. Ceram. Soc.*, **67** [12] C259-C260 (1984).
- ⁶D. Chakraborty and J. Mukerji, *J. Mat. Sci.*, **15** (1981) 3051-3056.
- ⁷K. Niihara and T. Hirai, *J. Mat. Sci.*, **12** (1977) 1243-1252.
- ⁸L. E. Davis, N. C. MacDonald, P. W. Palmberg, G. E. Riach, and R. E. Weber, *Handbook of Auger Electron Spectroscopy*, 2nd Edition, Physical Electronics Industry, Eden Prairie, MN 1972.

Table I. Vickers Microhardness of Fibers and Matrix (GPa)*

Load (N)	Matrix #			Fiber #		
	1	2	3	1	2	3
0.5	13.1±1.8	13.7±3.0	8.8±1.0	17.5±2.0	19.7±3.0	17.7±1.5
1.0	10.9±1.0	12.1±1.0	8.7±0.7	15.9±1.3	15.7±0.5	17.7±0.8
2.0	7.6±1.5	9.5±1.0	6.3±0.6	—	—	—

*Matrix (i) contains Fiber (i).

Table II. Chemical and Phase Composition of Mullite Fibers

Mullite Fibers	Chemical composition			Phase composition
	Al ₂ O ₃ wt%	SiO ₂ wt%	B ₂ O ₃ wt%	
Nextel 480				
nominal	70	28	2	Mullite (3Al ₂ O ₃ ·2SiO ₂)
present study*	70.1±1	29.9±1	nd*	Mullite (VS) [‡] +Amorphous phase (VW)
Nextel 440				
nominal	70	28	2	Mullite + γ -Al ₂ O ₃
present study*	69.6±1	30.1±1	nd*	Mullite (M-S) + η -Al ₂ O ₃ (S) + Amorphous phase (M-W)
Nextel 440 w/ C				
nominal	70	28	2	Mullite + γ -Al ₂ O ₃
present study*	70.5±1	29.5±1	nd*	Mullite (S) + η -Al ₂ O ₃ (S) +Amorphous phase (W)

*Corrected as explained in text.

*Not detected.

[‡]VS-Very Strong, S-Strong, M-Medium, W-Weak, VW-Very Weak.

Table III. Auger Peak Locations in Composite vs Handbook Values

Element	Composite location (eV)	Handbook value and environment (eV) [§]
Si	92	72 (Si), 76 (SiO ₂)
	1619	1619 (Si), 1606 (SiO ₂)
Al	68	51 (Al ₂ O ₃), 68 (Al)
	1394	1378 (Al ₂ O ₃), 1396 (Al)
C	272	272 (C)
B	179	179 (B)
O	508	503 (MgO)

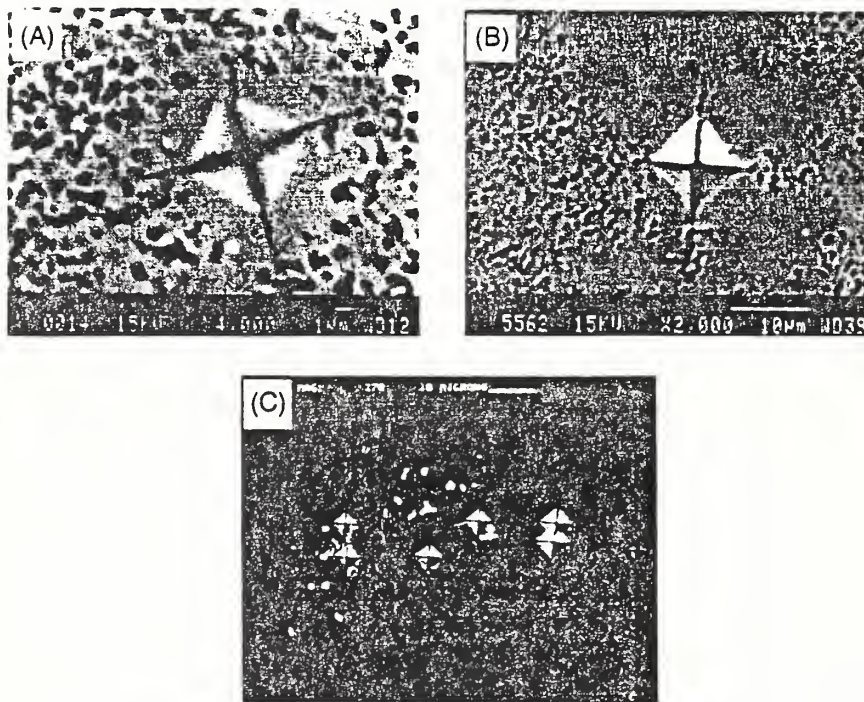


Fig. 1. Micrographs of polished and indented sections: (A) carbon-coated Nextel 440, 0.5 N load, (B) Nextel 440, 1.0 N load, and (C) Nextel 480, 1.0 N load.

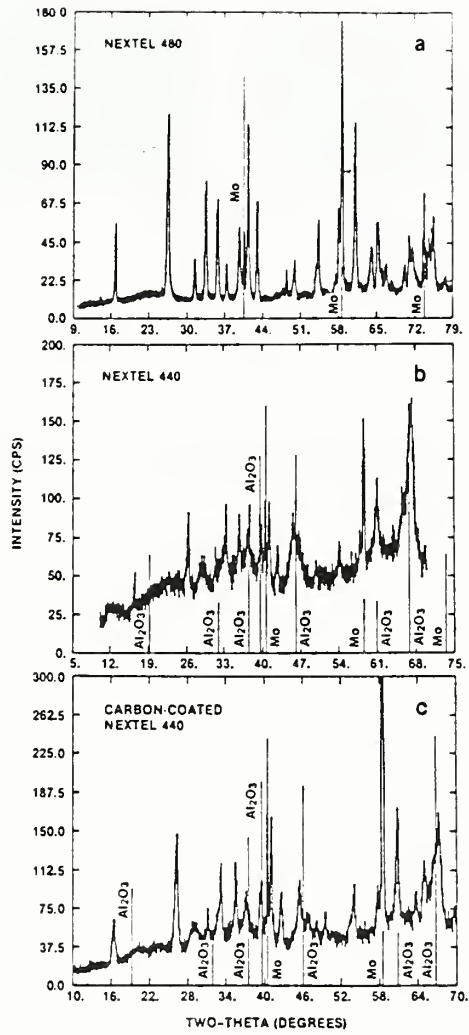


Fig. 2. X-ray diffraction patterns of the fibers on a Mo substrate (unmarked peaks are mullite): (A) Nextel 480, (B) Nextel 440, and (C) carbon-coated Nextel 440.

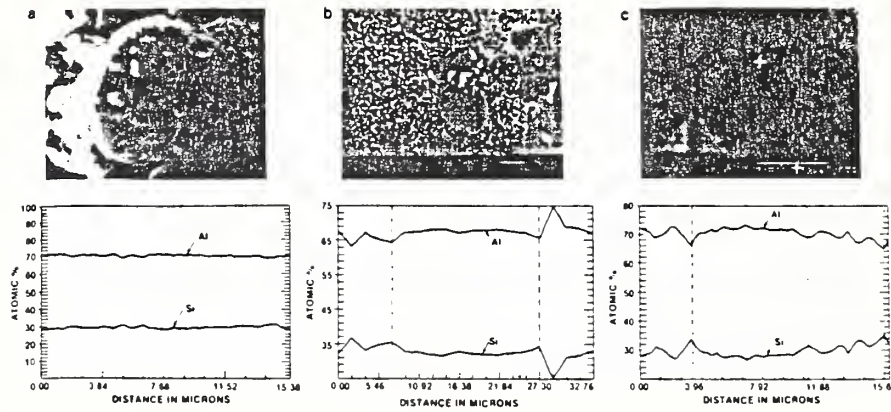


Fig. 3. EDX line scans showing Al and Si concentrations: (A) bare Nextel 480 fiber, (B) two Nextel 480 fibers in contact in composite, and (C) one Nextel 440 fiber in composite.

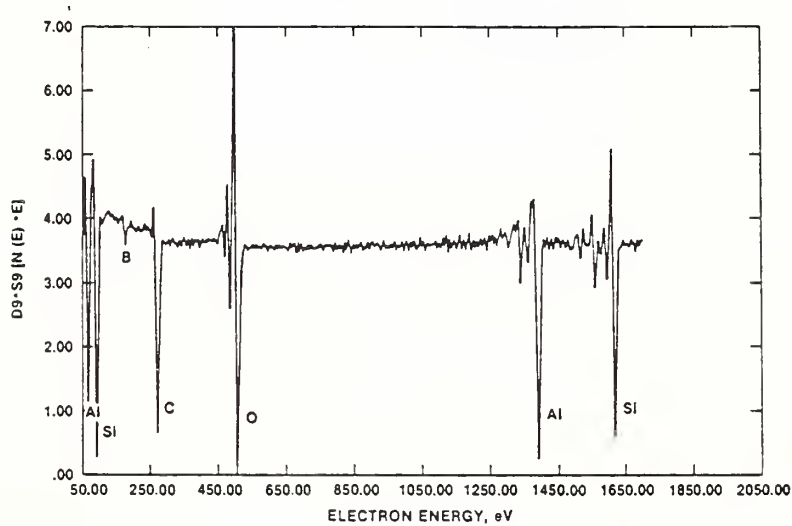


Fig. 4. AES survey scan of carbon-coated Nextel 440 fiber.

U.S. DEPT. OF COMM. BIBLIOGRAPHIC DATA SHEET <i>(See instructions)</i>	1. PUBLICATION OR REPORT NO. NISTIR 89-4073	2. Performing Organ. Report No.	3. Publication Date APRIL 1989
4. TITLE AND SUBTITLE Mechanical Property Enhancement in Ceramic Matrix Composites			
5. AUTHOR(S) S. W. Freiman, D. C. Cranmer, E. R. Fuller, Jr., and W. Haller			
6. PERFORMING ORGANIZATION <i>(If joint or other than NBS, see instructions)</i> NATIONAL BUREAU OF STANDARDS U.S. DEPARTMENT OF COMMERCE GAITHERSBURG, MD 20899		7. Contract/Grant No. N00014-86-F-0096 8. Type of Report & Period Covered Interim 1 Jan 88 to 31 Dec 88	
9. SPONSORING ORGANIZATION NAME AND COMPLETE ADDRESS <i>(Street, City, State, ZIP)</i> SDIO/IST C/O Office of Naval Research 800 N. Quincy Ave. Arlington, VA			
10. SUPPLEMENTARY NOTES <input type="checkbox"/> Document describes a computer program; SF-185, FIPS Software Summary, is attached.			
11. ABSTRACT <i>(A 200-word or less factual summary of most significant information. If document includes a significant bibliography or literature survey, mention it here)</i> The fiber-matrix interfacial properties of several glass and ceramic matrix composites have been determined using two indentation techniques and a single fiber pull-out technique. An instrumented indenter was developed to improve the acquisition and analysis of the data. The effects of thermal expansion mismatch were determined from three model composite systems containing large SiC monofilaments using the single fiber pull-out test. An indentation push-out test was successfully used to determine the debond strength of a borosilicate matrix/SiC monofilament/carbon core material. A comparison of the various techniques for determining the fiber-matrix interfacial properties was conducted.			
12. KEY WORDS <i>(Six to twelve entries; alphabetical order; capitalize only proper names; and separate key words by semicolons)</i> ceramics; ceramics composites; composites; fiber pull-out; fiber push-in; fiber push-out; mechanical properties fiber/matrix interfaces; interfacial strength; debond strength			
13. AVAILABILITY <input checked="" type="checkbox"/> Unlimited <input type="checkbox"/> For Official Distribution. Do Not Release to NTIS <input type="checkbox"/> Order From Superintendent of Documents, U.S. Government Printing Office, Washington, D.C. 20402. <input checked="" type="checkbox"/> Order From National Technical Information Service (NTIS), Springfield, VA. 22161		14. NO. OF PRINTED PAGES 80 15. Price \$14.95	

